MARTIN MARIETTA ENERGY SYSTEMS LIBRARIES

3 4456 0350971 8

AD_____

ORNL/TM-12097

ornl

OAK RIDGE NATIONAL LABORATORY

MARTIN MARIETTA

PREDICTIVE MODELLING AND LABORATORY STUDY OF ADHESIVE JOINT DETERIORATION IN THE M829 APFSDS KINETIC ENERGY ROUND[1]

FINAL REPORT

December 23, 1991

Date Published: April, 1992

Prepared for

Product Assurance Directorate
U. S. Army Armament Munitions
and Chemical Command
Picatinny Arsenal
Dover, New Jersey 07801

by

W. H. Griest, C. K. Bayne, J. E. Caton, R. Baldwin,
J. H. Moneyhun, W. M. Caldwell, and H. E. McCoy
Oak Ridge National Laboratory
Oak Ridge, Tennessee 37831

and

W. M. Nance, Jr.
Martin Marietta Ordnance Systems, Inc.
Milan Army Ammunition Plant
Milan, Tennessee 38358

OAK RIDGE NATIONAL LABORATORY
CENTRAL RESEARCH LIBRARY
CIRCULATION SECTION
4500N ROOM 175
LIBRARY LOAN COPY
DO NOT TRANSFER TO ANOTHER PERSON
If you wish someone else to see this report, send in name with report and the library will arrange a loan.

[1]Research sponsored by the U. S. Army Armament, Munitions, and Chemical Command, under U. S. Department of Energy Contract DE-AC05-84OR-21400 with Martin Marietta Energy Systems, Inc.

MANAGED BY
MARTIN MARIETTA ENERGY SYSTEMS, INC.
FOR THE UNITED STATES
DEPARTMENT OF ENERGY

This report was prepared as an account of work sponsored by an agency of the United States Government. Neither the United States Government nor any agency thereof, nor any of their employees, makes any warranty, express or implied, or assumes any legal liability or responsibility for the accuracy, completeness, or usefulness of any information, apparatus, product, or process disclosed, or represents that its use would not infringe privately owned rights. Reference herein to any specific commercial product, process, or service by trade name, trademark, manufacturer, or otherwise, does not necessarily constitute or imply its endorsement, recommendation, or favoring by the United States Government or any agency thereof. The views and opinions of authors expressed herein do not necessarily state or reflect those of the United States Government or any agency thereof.

EXECUTIVE SUMMARY

Field reports of the deterioration of combustible cartridge case wall material and adhesive joint ("skive joint") strength in the M829 APFSDS kinetic energy round, although infrequent, indicate the need for predictive surveillance of this munition component.

The main objective of this study was to develop a mathematical model of the skive joint strength which would allow prediction of the useful field service lifetimes of the M829 under any given set of exposure conditions and which could be used to define limits for storage conditions. A secondary objective addressed the case wall strength. These objectives were approached in a two-task study. Laboratory studies using coupons cut from the M829 case wall identified important variables and factors affecting adhesive joint and case wall strength. Accelerated environmental exposures and physical tests of full-up M829 rounds provided the data base from which predictive models were constructed.

Laboratory studies with combustible cartridge case coupons identified the importance of the external factors of humidity at high % relative humidity (% RH) and at elevated temperatures (ca. $\geq$ 50°C) to deterioration. Exposure effects at high temperatures were not completely reversible, probably from partial hydrolysis of the nitrocellulose polymer. Propellant effects also appeared to be important internal factors, but only at elevated temperatures or under leaching conditions (i.e., when a round is lying in a pool of water). Nitrogen oxide evolution and nitroester migration were two of the factors involved in propellant-related deterioration effects. Salt water, diesel and turbine fuels, hydraulic fluid, grease, and heavy lubricating oil did not cause significant deterioration under limited exposures, but CLP Cleaner did cause deterioration. Ketones were found to cause adhesive solvation and disbonding, suggesting that degreasing agents and paint removers should not be used near combustible cartridge cased munitions. The industrial pollutants sulfur dioxide and nitrogen dioxide under dry exposure conditions had no measurable effects. Nitric acid vapors were quite damaging, indicating that the acid forms of these pollutants could deteriorate the case wall and skive joint.

Tensile strength data from accelerated environmental exposures and physical testing of full-up M829 rounds were modelled using a number of approaches. The best mathematical fit was achieved using a logistic model, but predictions of skive joint lifetimes were shorter than expected from field experiences. The main factor limiting the precision of the models was round-to-round variability in the tensile strength. At the time the predicted average strength was 0 lbs (disbonding of the skive joint), the uncertainty was ca. 1,100 lbs. A kinetic model constructed from a selected subset of data predicted longer lifetimes, but uncertainties were still very large and humidity effects were not considered. Comparison of data for control M829 rounds and lot acceptance tests of surrogate case/adapter assemblies suggested that the additional manufacturing steps in the full-up M829 production introduce some of the variability.

MARTIN MARIETTA ENERGY SYSTEMS LIBRARIES

3 4456 0350971 8

Any model or any study of the M829 skive joint strength will be limited by the fundamental round-to-round variability in skive joint strength. This underlines the need for an engineering study to improve the design and production of the adhesive joint. It is suggested that the M829A1 be used in future predictive modelling studies, and that a time-to-failure protocol be tested for predictive success.

TABLE OF CONTENTS

EXECUTIVE SUMMARY 1

TABLE OF CONTENTS 3

LIST OF TABLES 4

LIST OF FIGURES 6

1. INTRODUCTION 8

2. SUPPORTING LABORATORY STUDIES 10

   2.1 Preliminary Tests of Solvents, Fuel, Water, and Salt 12
   2.2 Tests of Fuels, Lubricants, Cleaner, and Other Military Specification Fluids 14
   2.3 Tests of Temperature and Humidity Effects 17
   2.4 Tests of Propellant Effects 23
   2.5 Tests of Industrial Pollutants Effects 28

3. ACCELERATED ENVIRONMENTAL EXPOSURE OF FULL-UP M829 ROUNDS AND DEVELOPMENT OF PREDICTIVE MODELS 31

   3.1 Accelerated Environmental Exposure Experiment 31
   3.2 Results of Accelerated Environmental Exposures 33
   3.3 Predictive Models of Skive Joint Tensile Strength 36
   3.4 Comparison with Tensile Strength Data from Lot Acceptance Testing 46
   3.5 M829 Case Wall Indentation Hardness 49
   3.6 Nitroester Migration into the M829 Case Wall 50

4. CONCLUSIONS AND RECOMMENDATIONS 56

5. ACKNOWLEDGEMENT 58

6. REFERENCES 59

7. DISTRIBUTION LIST 61

LIST OF TABLES

Table 2.1. Effects of Water, Solvents, Fuel, and Nitric Acid Vapors on Coupon Wall Indentation Hardness and Adhesive Joint Tensile Strength. 13

Table 2.2. Effects of Coupon Exposure to Water or Salt Water, and Recovery for Exposure to Water. 14

Table 2.3. Effects of the Exposure of Coupons to Military Specification Fuels, Lubricants, Cleaner, and Fluid. 16

Table 2.4. Tensile Strength Data for Accelerated Environmental Exposures of Combustible Cartridge Case Coupons. 18

Table 2.5. Coefficients and Regression Statistics for TS = A + B*log(day + 1). 19

Table 2.6. Effects of Temperature and Humidity on Case Wall Indentation Hardness. 22

Table 2.7. Effects of Exposure to 50°C/97% RH with and without JA-2 Propellant. 25

Table 2.8. Effects of Soaking in Water and Water Plus JA-2 Propellant for 56 Days. 25

Table 2.9. Tensile Strength Data (lbs/in) for Honeywell Temperature Exposure of Coupons with and Without JA-2 Propellant. 26

Table 2.10. Propellant Effects for Each Exposure Temperature. 28

Table 2.11. Effects of Sulfur Dioxide and Nitrogen Dioxide Exposures. 30

Table 3.1. Levels of the Environmental Factors for the Central Composite Design. 32

Table 3.2. Tensile Strength Data from the Accelerated Environmental Exposure Experiment. 35

Table 3.3. Logistic Model Coefficients Estimated by Non-linear Least Squares. 38

Table 3.4. Tensile Strength Data Used to Estimate Rate Constants. 43

Table 3.5. Rate Constants Estimated from the Linear Regression of $(TS_0 - TS) = Kt$. 43

Table 3.6. Estimated Rate Constants and Lifetimes for Temperatures 20° C to 80° C. 46

Table 3.7. Tensile Strength (lbs) Summary Statistics for MAAP Lot Acceptance Tests. 48

Table 3.8. Case Wall Indentation Hardness for Selected Accelerated Environmental Exposures. 50

Table 3.9. Uniformity of Nitroester and Stabilizer Distribution in Nitrocellulose Wall at the Skive Joint. 52

Table 3.10. Results for Nitroester and Akradite II Measurements in M829 Nitrocellulose Case Wall at the Skive Joint after Accelerated Environmental Exposures. 53

LIST OF FIGURES

Fig. 1.1. Diagram of the 120 mm M829 APFSDS Kinetic Energy Round 9

Fig. 2.1. Combustible Cartridge Case Coupons from the M829 Case Wall 11

Fig. 2.2 Predicted Tensile Strength (lbs/in) for Combustible Cartridge Case Coupons. 20

Fig. 3.1. Central Composite Design for the Accelerated Environmental Exposures of M829 Rounds. 32

Fig. 3.2. M829 Case Wall Sections Taken just below the Skive Joint after Accelerated Environmental Testing. 34

Fig. 3.3. Tensile Strength Data Ordered by Increasing Average Value. 37

Fig. 3.4. Logistic Model Response Surface for Tensile Strength Estimated at Week 12. 39

Fig. 3.5. Predicted Tensile Strengths with 95% Confidence Intervals for Exposure at 21°C and 80% RH. 40

Fig. 3.6. Predicted Tensile Strengths with 95% Confidence Intervals for Exposure at 35°C and 50% RH. 41

Fig. 3.7. Predicted Tensile Strengths with 95% Confidence Intervals for Exposure at 66°C and 90% RH. 41

Fig. 3.8. Linear Regression of (TS_0 - TS) vs Kt. 44

Fig. 3.9. Arrhenius Plot of Rate Constants. 45

Fig. 3.10. Histogram of 157 Tensile Strengths from M829 Lot Acceptance Tests at the MAAP. 47

Fig. 3.11. Box Plots and Quality Control Chart for MAAP Lot Acceptance Tests. 49

Fig. 3.12. Plot of Total Nitroester Concentration Versus Skive Joint Tensile Strength in M829 Rounds from Accelerated Environmental Exposures. 55

1. INTRODUCTION

The 120 mm M829 APFSDS kinetic energy round (Figure 1.1) is a unique munition fired in the main gun of the M1A1 Abrams main battle tank. This round features a combustible cartridge case which is consumed upon firing, and only the metal base remains for disposal. This considerably reduces the crew compartment clutter normally resulting from a full steel cased round.

One critical feature of this round is the adhesive joint (called the skive joint in the M829) between the combustible cartridge case and the cellulosic adapter cone which holds the penetrator assembly in place. Reports from the field have indicated two rare but potentially important problems with the combustible cartridge case: disbonding of the adhesive joint with loss of the penetrator assembly, and crumbling of the case wall during handling. Although these problems have been infrequent, they indicate the need for predictive surveillance of this munition feature. Studies at the U. S. Army Armament, Munitions, and Chemical Command (AMCCOM) (1,2) and Honeywell (3) identified the external variable of temperature and the secondary internal effect of propellant nitroester migration as important contributors to skive joint deterioration and failure. Studies of accelerated environmental exposures with measurements of nitroester migration rate and skive joint deterioration predicted field service lifetimes of 4.8 (2) to 8.6 (3) years under mild (ca. 21°C) conditions. These studies suggested the feasibility of constructing a mathematical model for field service lifetime prediction. Fitting a full second-order response surface model with terms in temperature in °C (T) and time in days (D) to the AMCCOM data, and eliminating terms which were not significantly different than zero, the following equation for adhesive joint strength (in coupons cut from exposed surrogate rounds) was obtained:

$$\text{Tensile Strength (lbs/in)} = 122.16 + 9.49T - 0.1150\,T^2 - 0.0426\,TD$$

The model suggested that temperature had a more important effect on adhesive joint strength than time, under the conditions of the AMCCOM study. On the basis of this pioneering work, a more detailed study was designed.

The main objective of this study was to develop a mathematical model of the M829 skive joint strength which would allow prediction of the useful field service lifetimes of the M829 under any given set of exposure conditions and which could be used to define limits for storage conditions. A secondary objective addressed the case wall strength. These objectives were approached in a two task study. Laboratory studies using coupons cut from the M829 case wall identified important variables and factors affecting adhesive joint and case wall strength. These studies are reported in Chapter 2. Accelerated environmental exposures and physical tests of full-up M829 rounds provided the data base from which predictive models were constructed. These studies are described in Chapter 3.

Fig. 1.1. Diagram of the 120 mm M829 APFSDS Kinetic Energy Round

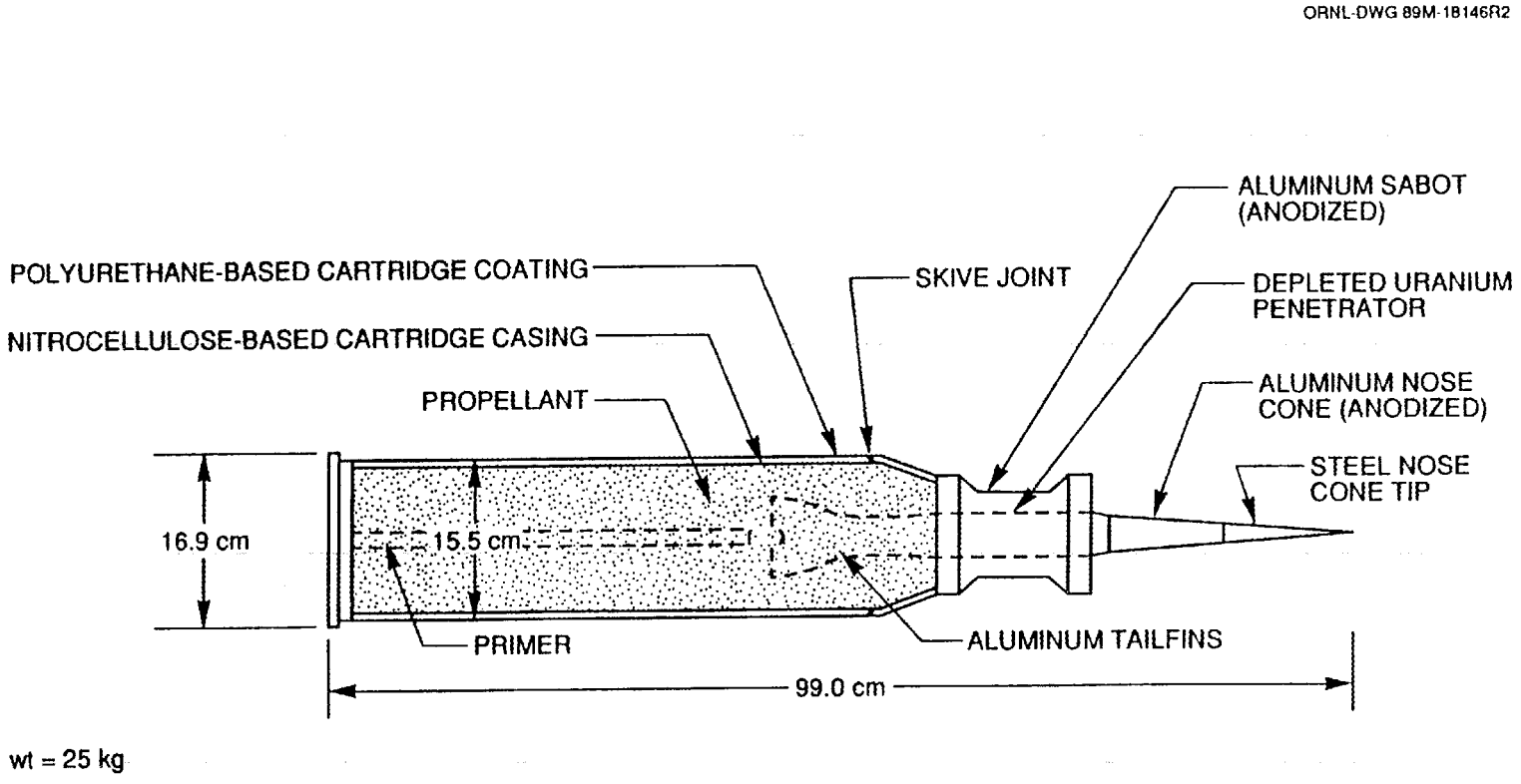

2. SUPPORTING LABORATORY STUDIES

Laboratory studies were designed to determine what exposure factors and conditions are important to the deterioration of the nitrocellulose case wall and skive joint in the M829 round and other munitions having the same materials of construction, and to facilitate the understanding needed to interpret the results of the accelerated exposures with full-up M829 rounds. Important factors or variables were to be identified for potential future study with the full-up rounds, and factors or variables not influencing the case wall or adhesive joint could be identified and dismissed as not requiring further study.

Combustible cartridge case coupons were used in the laboratory studies. They have been found useful in previous work (3) as relatively inexpensive surrogates for studying the behavior of the skive joint in the full-up M829 round. The composition of the combustible cartridge case wall and adapter cone are listed below:

Combustible Cartridge Case Wall:

57.2% Nitrocellulose (13.4% N)
31.0% Kraft Wood Fiber
11.0% Polyurethane Resin
0.8% Akradite II (methyldiphenyl urea stabilizer)

Adapter Cone:

61.0% Kraft Wood Fiber
27.0% Wood Fiber
12.0% Polyurethane

Adhesive (before curing):

26% solution of nitrocellulose in ethanol, acetone, butyl acetate, and methyl abietate

As illustrated in Figure 2.1, coupons consisted of 2.5 cm x 15 cm strips which were cut longitudinally from the wall of bonded case/adapter cone assemblies, and centered around the adhesive joint. Uncoated components purchased from Armtec (Coachella, CA) were bonded with military specification nitrocellulose adhesive on the M829 production line at the Milan Army Ammunition Plant (MAAP, Milan, TN). The coupons were carefully cut from the cured assemblies and were individually numbered and stored by round number in plastic bags. The bagged coupons were stored in a type 2 explosives magazine under ambient laboratory conditions (ca. 21°C/40% RH).

Fig. 2.1. Combustible Cartridge Case Coupons from the M829 Case Wall

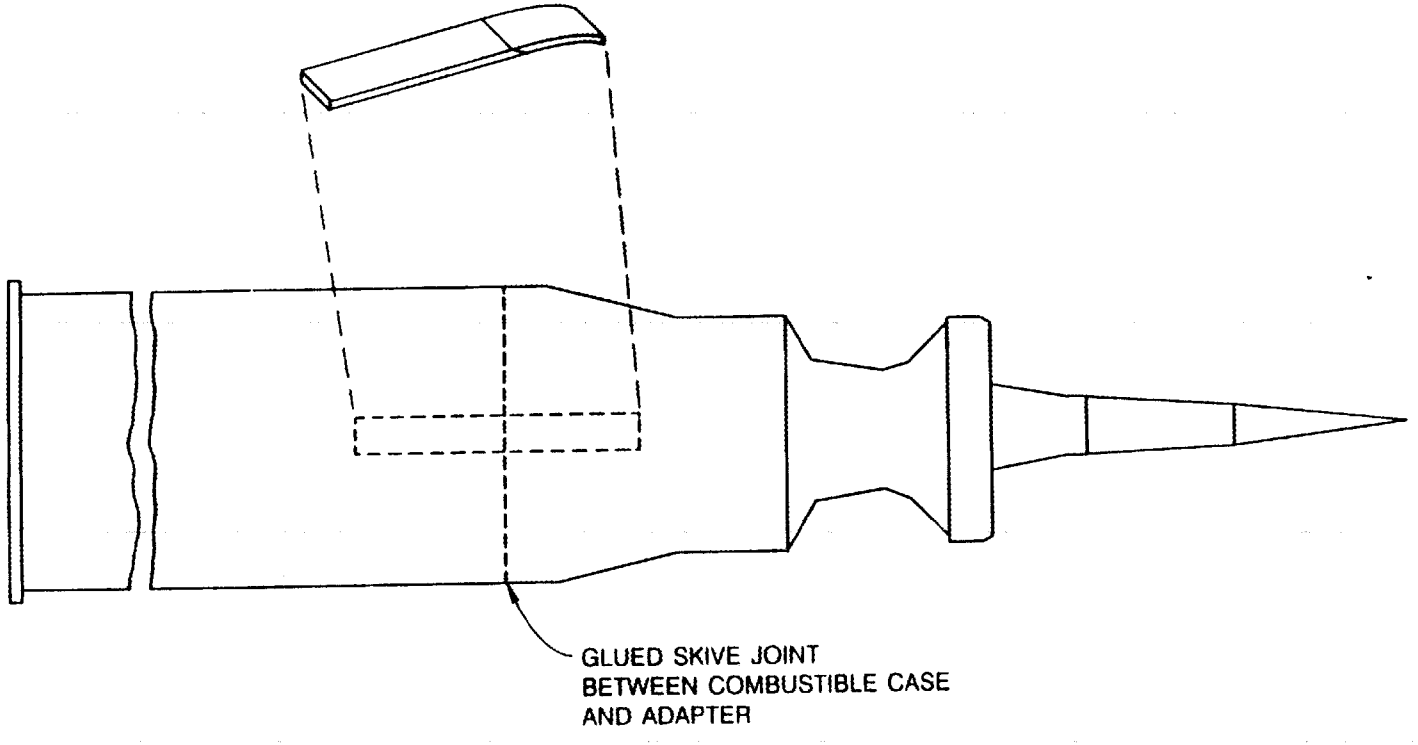

The coupons were subjected to various exposures and the effects were determined by two physical tests. Influences on case wall indentation hardness were quantified using a D-scale durometer. The hardness was measured at four points along the nitrocellulose side of the coupons before and after the exposures. The tensile strength of the adhesive joint was measured only after exposure because this is a destructive test. A simple methodology was devised for achieving a straight-line pull on the adhesive joint in the determination of the tensile strength. The angled portion of the adapter end of the coupon was cut off, leaving ca. 2 - 3 cm to grip in the holder of the test apparatus. Epoxied blocks or specially machined holding fixtures were not needed. An Instron tensile test machine was used for the tests, with a crosshead speed of 0.05 in/min. This strain rate was chosen because measured fracture loads at speeds of 0.5 in/min (208 $\pm$ 25.2 lbs/in) and 0.005 in/min (183 $\pm$ 28.1 lbs/in) were the same as at 0.05 in/min (206 $\pm$ 22.2 lbs/in). The test data were calculated in units of lbs/in rather than the conventional lbs/in^2 to allow comparison with previous studies.

The first two sets of experiments explored the effects of solvents, water, and other chemicals to which the full-up rounds could conceivably be exposed during production, storage, or deployment.

2.1 Preliminary Tests of Solvents, Fuel, Water, and Salt

The first set of experiments tested the effects of coupon exposures to vapors of various chemicals or fuel. Two coupons were sealed in a 1 L glass bottle with a Teflon-lined screw cap. A small vial containing ca. 20 mL of the test fluid was placed in the bottle to provide vapor exposure. The sealed jars were stored at ambient room temperature (ca. 21°C) in an explosion-shielding box constructed from 2.5 cm thick Lexan. Water, number 2 diesel fuel (DF-2), acetone, xylene, and nitric acid were tested for ca. 2 weeks. The DF-2 was tested for an additional period because exposure of full-up rounds to transportation fuel vapors was considered to be important. The data from the physical tests of the coupons after exposure and of control coupons stored in the explosives magazine are listed in Table 2.1.

It was apparent that acetone, a ketone, quickly caused the adhesive to solvate and disbond. This is not surprising, because acetone is a solvent in the wet adhesive solution. Methylethyl ketone is often used as a degreasing agent on munitions production lines. It should not be used near munitions with such adhesive joints because these results show they can be rapidly degraded by exposure to ketone vapors. The nitric acid also had a strong effect. The case wall was discolored, probably from nitration of the Akardite II stabilizer, to form colored nitrodiphenylamines. It also attacked the nitrocellulose, which softened and became crumbly. This suggests that oxides of nitrogen, when combined with water vapor to form acids, can cause deterioration of the adhesive joint and case wall. Oxides of nitrogen arise from propellant ageing and decomposition (4) or industrial pollutants.

The mode of break in all the tensile tests of the adhesive joints was cohesive failure in the layer of nitrocellulose immediately below the adhesive, which suggests that the case wall material penetrated by the adhesive was weakened by the exposures. All disbonding (tensile strength = 0) was, of course, adhesive failure.

Table 2.1 Effects of Water, Solvents, Fuel, and Nitric Acid Vapors on Coupon Wall Indentation Hardness and Adhesive Joint Tensile Strength. (Avg. for n = 2)

Chemical	Length of Exposure, Days	Ind. Hardness, D-scale		Tensile Strength, lbs/in
		Initial	Final	
Water	17	70	60	128
DF-2	17	70	68	220
	91	64	69	221
Acetone	1	70	26	0[1]
Xylene	14	65	68	225
Nitric Acid	52	70	59	49.9
Control	17	71	71	207
	91	67	69	220

[1]Adhesive joint disbonded within 27 hrs.

Water vapor also exhibited an effect. This was explored further in a test which included salt, to test the potential effects of the exposure of munitions to sea spray. Salt causes severe corrosion of depleted uranium penetrators, and it was important to determine effects on the cartridge case wall and adhesive joint. For this test, 8 coupons were soaked in either distilled water or a 3.5% (wt/vol) solution of sodium chloride in water. The coupons were then sealed in a jar with a puddle of water and a filter paper wick to maintain saturated humidity. The jars were stored as described above. Two extra coupons from the water exposure were allowed to dry under ambient laboratory conditions for 66 days to test for recovery from the exposure to water. The results of the physical tests are presented in Table 2.2.

Table 2.2. Effects of Coupon Exposure to Water or Salt Water, and Recovery for Exposure to Water. (Avg. ± Std. Dev. for n = 4, except for recovery experiment and control with n = 2).

Exposure	Exposure or Recovery, Days	Ind. Hardness, D-scale		Tensile Strength, lbs/in
		Initial	Final	
Water	52	71 ±2.3	61 ± 2.6	153 ± 13.5
Recovery	66	70	68	274
Salt Water	52	71 ± 2.4	59 ± 1.8	148 ± 22.2
Control	52	72	70	316

This test confirmed that water significantly softens the case wall and weakens the adhesive joint. However, the effect is reversible, suggesting that only a simple hydration of the nitrocellulose occurred. The effects of salt water were indistinguishable from those of pure water under these conditions. This is consistent with the expectation that salt should not have a chemical interaction with nitrocellulose under mild exposure conditions. Humidity effects were tested further, and are described in section 2.3.

2.2 Tests of Fuels, Lubricants, Cleaner, and Other Military Specification Fluids

The preliminary experiments (described in section 2.1) showed that water and certain chemicals could deteriorate the case wall and adhesive joint. As a follow-up, common fluids to which full-up rounds could be exposed in the field were tested next. In these tests, four coupons were soaked in the fluid (or smeared with the grease) for 10 min. The coupons were then allowed to drain onto a paper towel, and then were sealed in glass jars which had the drain towels crumpled on the bottom to maintain a vapor exposure to the fluid. The physical testing data are reported in Table 2.3.

Only the CLP Cleaner appeared to have caused a significant deterioration of the adhesive joint strength, but the case wall indentation hardness was not affected appreciably. This suggests that the main effect was upon the adhesive or nitrocellulose wall penetrated by the adhesive, and not the polyurethane coating or bulk nitrocellulose wall material. The results for 73 days of exposure were the same as for 17 days, which suggests that the deterioration resulted mainly from the soaking, and that the vapors had little, if any, effect.

The DF-2 and turret hydraulic fluid also appear to have had a slight effect on adhesive joint tensile strength, but the values are very close to the lower limit of the uncertainty about the tensile strength averaged over all control coupons used in this study (234 $\pm$ 42 lbs/in), and thus they probably are not significant effects. Nuclear, biological, and chemical warfare agent (NBC) decontamination chemicals were not tested in this study, and they should be included in future work.

Table 2.3. Effects of the Exposure of Coupons to Military Specification Fuels, Lubricants, Cleaner, and Fluid. (Avg. for n = 2)

Substance	Military Specification	Period of Exposure, Days	Ind. Hardness, D-scale		Tensile Strength, lbs/in
			Initial	Final	
Grease	MIL-G-10924F	17	69	67	252
		73	65	65	321
Jet A-1 Turbine Fuel		17	70	72	236
		73	70	67	195
Engine/Transmission Oil	MIL-L-2104C	17	71	71	217
		73	67	67	217
CLP Cleaner	MIL-L-6360C	17	69	64	102
		73	71	67	122
Turret Hydraulic Fluid	MIL-H-46170	17	69	67	190
		73	70	65	203
DF-2		17	68	67	181
		73	68	68	181
Control		17	70	69	287
		73	68	65	193

2.3 Tests of Temperature and Humidity Effects

The experiments described in section 2.2 demonstrated effects of water soaking and humidity on the case wall and adhesive joint. Studies at AMCCOM (1,2) and Honeywell (3) showed that temperature is an important external factor in skive joint deterioration. Therefore, a study was made of the combined effects of temperature and humidity. The use of coupons allowed those effects to be studied independently of secondary internal effects arising from the propellant (i.e., nitrogen oxides evolution and nitroester migration).

Temperature and humidity effects were studied at room temperature and at elevated temperatures. The former were conducted in large glass desiccators which were kept in the Lexan explosive shields. Humidity was controlled by placing Drierite desiccant (for ca. 5% RH), saturated dipotassium hydrogen phosphate (70% RH), or distilled water (ca. 97 to 100% RH) in the bottom of the desiccators. Humidity was monitored using membrane-type humidity meters which were calibrated with a wet bulb/dry bulb hygrometer. The exposures at elevated temperatures were conducted using a custom designed and constructed explosion-proof temperature/humidity chamber from Tenney Engineering, Inc. (Union, NJ). The custom chamber was based upon their model T10 chamber.

The results of the experiments are divided into two sections (adhesive joint effects and case wall hardness effects) even though the experiments were conducted together.

Adhesive Joint Tensile Strength Effects:

Two series of experiments were conducted to examine temperature and humidity effects:

1. Three different humidities (ca. 0-5%, 70%, and 97-100% RH) at room temperature (ca. 21°C), and two humidities (21% and 97-100% RH) at 85°C to examine humidity effects.

2. Three different temperatures and humidities (50°C/97% RH, 70°C/38% RH, and 85°C/21% RH) which correspond to the same vapor pressure of water (0.118 atm) to isolate temperature effects from water vapor pressure. It is assumed that the vapor pressure of water is the critical factor. Vapor pressures are used in kinetic expressions for gas - solid reactions.

The results from these experiments are listed in Table 2.4.

Table 2.4. Tensile Strength Data for Accelerated Environmental Exposures of Combustible Cartridge Case Coupons.

Obs	Temp. (°C)	Relative Humidity (%)	Day	Replicate tensile strengths (lbs/in) #1	#2	#3	#4	Reps	Average	Standard Deviation
1	21	5	14	245.0	227.0	265.0	.	3	245.667	19.0088
2	21	5	25	330.0	188.0	261.0	.	3	259.667	71.0094
3	21	5	56	239.0	192.0	278.0	.	3	236.333	43.0620
4	21	5	112	193.0	173.0	262.0	.	3	209.333	46.6940
5	21	5	231	287.0	153.0	306.0	.	3	248.667	83.3926
6	21	70	14	238.0	143.0	301.0	.	3	227.333	79.5383
7	21	70	25	289.0	213.0	242.0	.	3	248.000	38.3536
8	21	70	56	207.0	180.0	220.0	.	3	202.333	20.4042
9	21	70	112	213.0	251.0	316.0	.	3	260.000	52.0865
10	21	70	231	253.0	143.0	252.0	.	3	216.000	63.2218
11	21	97	14	173.0	183.0	190.0	.	3	182.000	8.5440
12	21	97	29	142.0	128.0	149.0	.	3	139.667	10.6927
13	21	97	56	116.0	105.0	115.0	.	3	112.000	6.0828
14	21	97	114	59.2	80.5	73.7	.	3	71.133	10.8795
15	21	97	224	56.3	46.7	45.0	.	3	49.333	6.0929
16	50	97	15	112.0	115.0	119.0	127.0	4	118.250	6.5000
17	50	97	28	113.0	111.0	114.0	120.0	4	114.500	3.8730
18	50	97	64	95.5	104.0	84.3	112.0	4	98.950	11.8649
19	70	38	16	216.0	227.0	218.0	231.0	4	223.000	7.1647
20	70	38	29	152.0	213.0	207.0	162.0	4	183.500	30.9677
21	70	38	57	182.0	175.0	162.0	144.0	4	165.750	16.7008
22	70	38	119	114.0	127.0	143.0	132.0	4	129.000	12.0277
23	85	21	14	131.0	117.0	142.0	134.0	4	131.000	10.4243
24	85	21	29	115.0	105.0	97.0	105.0	4	105.500	7.3711
25	85	21	56	99.5	37.4	50.8	35.8	4	55.875	29.8509
26	85	21	83	48.6	52.4	64.2	27.5	4	48.175	15.3002
27	85	97	3	147.0	112.0	106.0	.	3	121.667	22.1435
28	85	97	14	35.0	47.7	52.4	.	3	45.033	9.0013
29	85	97	21	24.7	26.5	28.3	.	3	26.500	1.8000
30	85	97	28	24.0	30.8	.	.	2	27.400	4.8083

The coupon adhesive joint tensile strength data were modelled. The prediction equation has the form (i.e., logarithm, base e):

$$Tensile\ Strength = A + B*\log(day+1).$$

Note that log(day + 1) = 0 if day = 0, therefore parameter "A" represents the initial response. This model can be tested for lack-of-fit by comparing the variation explained by the model with the variation estimated by replicate tensile strength measurements on the same day. This test indicated that no lack-of-fit could be detected for this model at either the 5% or 10% significance level for any of the exposure data sets.

The coefficient and regression statistics for the prediction equations are given in Table 2.5. Plots of the predictive equations are shown in Figure 2.2.

Table 2.5. Coefficients and Regression Statistics for TS = A + B*log(day + 1).

Temp (°C)	RH (%)	Intercept A	Slope B	St. Dev. Intercept	St. Dev Slope	$\%R^2$	St. Dev. Observation
21	5	266.5	-6.58	57.8	13.91	2	52.99
21	70	238.8	-2.00	57.7	13.88	0	52.88
21	97	311.6	-49.41	10.1	2.43	97	9.00
50	97	159.0	-14.09	14.1	4.04	55	8.04
70	38	347.8	-45.75	24.2	6.31	79	18.42
85	21	273.7	-51.73	25.3	6.84	80	17.90
85	97	191.2	-51.92	14.1	5.26	92	13.25

The slope B is the main parameter of interest. It is the rate of tensile strength deterioration in units of lbs/in per ln(days of exposure). The standard deviation of the slope permits comparison of the slopes. It is apparent that for room temperature exposures, the rates of deterioration are not different from each other or from 0 at 5% and 70% RH. The rate of deterioration is increased significantly at humidity near saturation (97% RH), indicating that RH is not important except at such high values. It is not clear why the observed rate of deterioration at 50°C/97% RH was lower than at 21°/97% RH, except that the data for 50°/97% RH did not make sense. Two separate experiments were run at this condition (data for second run are listed), and the first run yielded scattered data points showing no consistent trend. The rates at 70°C and 85°C were the same as at 21°C/97% RH, which suggests that at high temperatures, the RH and also water vapor pressure are not the dominant factors. This suggests that the water content even at the lowest % RH is sufficient, i.e., is saturating the reactive sites in the adhesive joint.

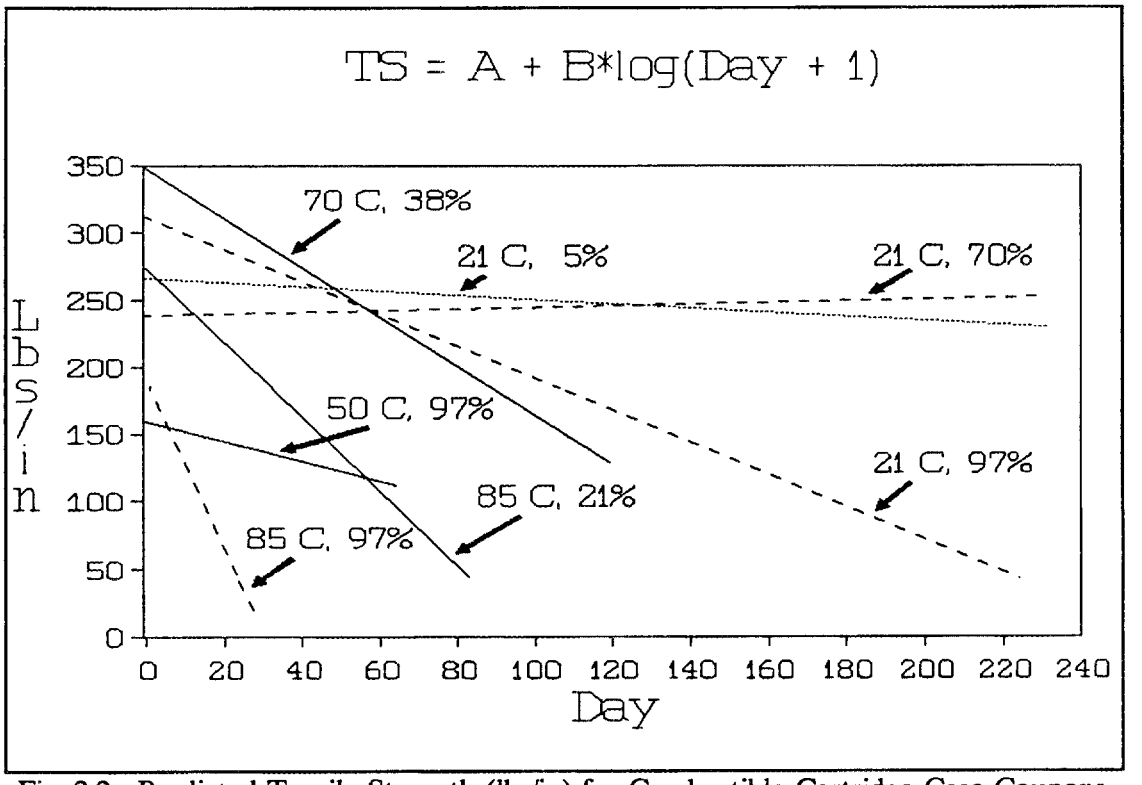

Fig. 2.2. Predicted Tensile Strength (lbs/in) for Combustible Cartridge Case Coupons.

Case Wall Indentation Hardness Effects:

Table 2.6 shows the effects of temperature and humidity on the case wall hardness. Except for 85°/21% RH and 70°/38% RH, data are not listed for the other exposures which had no significant effects on case wall hardness. The results indicate that, under the conditions of these coupon experiments, humidity effects were important only at high relative humidities. For example, case wall softening was observed only when the water vapor was near saturation at 85°, 50°, and 21°C. Case wall softening was not observed at 70°/38% RH or at 85°/21% RH, but softening was observed at 50°/97% RH, even though the water vapor pressure was the same (0.118 atm) for all 3 exposures. This suggests that the important parameter is how near water vapor is to saturation and not the absolute water vapor pressure. In contrast, the common kinetic convention is to use vapor pressure units in gas-solid reactions. This suggests that the tendency for the water to condense on or in the nitrocellulose is important.

The results also demonstrate the humidity effects are more severe at higher temperatures, and that softening at high temperatures and relative humidities are not reversible. This probably reflects processes such as hydrolysis and breakage of the nitrocellulose polymer.

Table 2.6. Effects of Temperature and Humidity on Case Wall Indentation Hardness. (Avg ± Std. Dev.)

Temp., °C	Humidity, %RH	Vapor Pressure, Atm.	Exposure, Days	Replicates	Ind. Hard., D-scale	
					Initial	Final
85	97	0.553	3	3	72 ± 1.2	63 ± 2.1
			14	3	71 ± 1.0	43 ± 1.7
			21	3	70 ± 2.6	38 ± 7.0
			28	2	72	43
			21 + Rec'y[1]	2		41
85	21	0.118	29	4	67 ± 1.0	67 ± 1.8
70	38	0.118	29	4	67 ± 2.4	67 ± 1.0
50	97	0.118	15	4	70 ± 1.3	61 ± 1.8
			28	4	70 ± 1.3	59 ± 1.4
			64	4	70 ± 1.3	59 ± 1.7
21	97	0.027	14	3	66 ± 1.5	62 ± 3.5
			29	3	66 ± 1.0	60 ± 1.2
			56	3	65 ± 1.5	55 ± 3.2
			114	3	65 ± 1.6	54 ± 3.8
			224	3	64 ± 3.8	44 ± 10

[1]Coupon dried to test recovery from exposure.

2.4 Tests of Propellant Effects

The full-up M829 round contains ca. 17 lbs of JA-2 propellant, which has the following specification:

59.5 ± 2%	Nitrocellulose (13.1 ± 0.1% N)
24.8 ± 1.5%	Diethyleneglycol dinitrate
14.9 ± 1%	Nitroglycerin
0.7 ± 0.2%	Methyldiphenyl urea
1.03 - 0.05%	Graphite
1.03 - 0.05%	Magnesium oxide
≤0.25%	Graphite glaze

Both AMCCOM (1,2) and Honeywell (3) reported that the secondary, internal factor of nitroester migration was an important contributor to skive joint disbonding. Therefore, experiments were designed to test propellant effects.

These tests included a part of the temperature and humidity experiments reported in section 2.3. Briefly, for the temperature/humidity tests conducted in the explosion-proof chamber, trials at 50°C/97% RH were conducted with and without JA-2 propellant. Coupons exposed without JA-2 propellant were simply laid on the shelves within the chamber. Coupons for JA-2 exposure were kept in contact with the propellant in a geometry similar to that in the full-up round. The 16 coupons and 160 g of propellant were sealed in a galvanized paint can which also contained a beaker of water to provide humidity. The can was kept in the exposure chamber. Inside the can, the coupons were held in a cylindrical arrangement around the outside of the beaker by bands of wire. A single layer of JA-2 propellant pellets separated the coupons and the beaker wall, but did not contact the full length of the coupons. Only the area of the coupon around the skive joint was in contact with the propellant. In these experiments, the case wall directly contacted the propellant, whereas in the full-up round, a silk propellant bag separated the propellant and case wall. Coupons were exposed for 15, 28, and 64 days. Additional coupons exposed for 64 days were allowed to dry in the explosion shield in a laboratory hood for 95 days to test recovery from the exposures.

The results of this experiment are listed in Table 2.7. In both exposures there was a significant softening of the case wall which was not completely recovered during the lengthy drying period. This suggests irreversible damage to the nitrocellulose, such as by a partial hydrolysis of the polymer. The coupons exposed to the JA-2 propellant were discolored where the propellant contacted the coupon, and in those discolored areas, the case wall was appreciably softer (55 D-scale hardness units). This shows a definite propellant effect. It is not clear why the tensile strengths of the temperature/humidity exposure were always lower (except after recovery) than for those exposures which included JA-2 propellant. It is possible that a greater mass of propellant should have been used, and the exposures run for longer periods to make propellant effects more pronounced.

Another experiment examined propellant effects simulating those of a full-up round soaking in a puddle of water. This experiment was prompted by field reports of ammunition handling and storage showing water marks on rounds and on the bottom row of the ready rack of the M1A1 turret bustle ammunition compartment. In these experiments, 6 coupons were sealed in glass jars filled with distilled water and 72 g of JA-2 propellant. As a control, another jar contained coupons and water only. The jars were stored in an explosives magazine for 8 weeks at ambient laboratory conditions (ca. 23° C). Three coupons were then withdrawn for physical testing, and 3 for drying in the explosion shield for 8 weeks before testing to examine recovery. The coupons which were exposed to JA-2 plus water turned a yellow color, while the coupons exposed to water only did not change color. This suggests that products from the propellant (possibly nitrates, nitrites, or nitrate esters) diffused from the propellant, through the water, and reacted with the nitrocellulose. The yellow color probably resulted from the formation of nitrodiphenylamines by reactions of propellant decomposition products with the Akardite II stabilizer in the case wall and propellant. Physical data for the exposure effects are listed in Table 2.8.

Both sets of coupons showed severe weakening of the adhesive joint (ca. 75% loss of strength) and softening of the case wall indentation hardness (ca. 24% loss of D-scale hardness). However, it was surprising that there were no significant differences between the specimens exposed to water alone and water plus JA-2 propellant. The indentation hardness of both sets of samples was recovered after 8 weeks of drying, indicating that the case wall deterioration was reversible. The tensile strength of the adhesive joints was fully recovered in the water exposure, but was not fully recovered in the JA-2 plus water exposure, suggesting that the area in the immediate vicinity of the joint did sustain a partially irreversible damage. This experiment did not demonstrate strong propellant effects, but it did suggest that full-up rounds which have soaked in water for appreciable periods could undergo irreversible deterioration.

Table 2.7. Effects of Exposure to 50°C/97% RH with and without JA-2 Propellant. (Avg. ± Std. Dev. for n = 4, except for Control with n = 2)

Exposure	Period of Exposure, Days	Ind.Hardness, D-scale			Tensile Strength, lbs/in
		Initial	Final	Recovery	
50°C/97%RH	15	70 ± 1.3	61 ± 1.8		118 ± 6.5
	28	70 ± 1.3	59 ± 1.4		115 ± 3.9
	64	70 ± 1.3	59 ± 1.7		99.0 ± 11.9
Exposure + Recovery	64 + 95	69 ± 2.2	61 ± 2.5	65 ± 1.3	177 ± 32.6
50°C/97% RH/JA-2	15	69 ± 2.3	62 ± 3.3		204 ± 43.0
	28	70 ± 1.0	62 ± 2.5		207 ± 31.3
	64	69 ± 1.5	63 ± 1.7		172 ± 37.2
Exposure + Recovery	64 + 95	70 ± 1.7	61 ± 1.0	62 ± 1.3	236 ± 35.0
Control	-	-	69		205

Table 2.8. Effects of Soaking in Water and Water Plus JA-2 Propellant for 56 Days. (Avg. ± Std. Dev. for n = 3, except for control with n = 4)

Exposure	Ind.Hardness, D-scale			Tensile Strength, lbs/in
	Initial	Final	Recovery	
Water Soak	70 ± 1.2	53 ± 0.6		53.3 ± 7.3
Exposure + Recovery	69 ± 1.2	49 ± 0.6	67 ± 2.1	259 ± 88.2
Water + JA-2 Soak	68 ± 0.6	50 ± 0.6		63.9 ± 16
Exposure + Recovery	68 ± 1.0	48 ± 0.6	65 ± 0.6	186 ± 29.5
Control	68 ± 1.8	66 ± 1.4		281 ± 56.4

A third examination of propellant effects used data published (3) by Honeywell for coupons exposed with and without JA-2 propellant to different temperatures. For these experiments, Honeywell sealed 2 to 4 coupons in 1-gallon paint cans with or without 1 lb of JA-2 propellant. The cans were stored at 20° to 85°C for periods of 2 to 364 days before tensile testing. This was part of a study comparing different polyurethane and nitrocellulose adhesives. Table 2.9 shows the Honeywell data from reference (3).

Table 2.9. Tensile Strength Data (lbs/in) for Honeywell Temperature Exposure of Coupons with and Without JA-2 Propellant. (Data from ref.3).

Data for Nitrocellulose, USA		Days Exposed to JA-2 Vapors								
		0	2	5	12	30	106	196	357	Avg
		Lbs/in	Lbs/in	Lbs/in	Lbs/in	Lbs/in	Lbs/in	Lbs/in	Lbs/in	Lbs/in
Temp., °C	JA-2 Exposure									
21	Without Propellant	309	.	.	256	310	264	.	246	277
	With Propellant	.	.	.	311	329	294	282	196	282
50	Without Propellant	.	.	219	272	208	233	.	176	222
	With Propellant	.	.	256	264	248	251	168	242	238
70	Without Propellant	.	210	204	244	193	154	.	78	181
	With Propellant	.	252	227	202	162	74	96	64	154
85	Without Propellant	.	244	196	163	143	.	.	.	187
	With Propellant	.	288	171	148	80	.	.	.	172

The effects of JA-2 propellant were compared by the "extra sum of squares" principle in linear regression (5). A single regression model was fitted to the data ignoring the propellant effect then two regression models were fitted to the data accounting for propellant effects. The extra sum of squares attributed to ignoring the propellant effects was calculated by subtracting the total sum of squares for the two separate models from the sum of squares for the single model. This "extra sum of squares" was tested by an F-test to see if the data set indicated a propellant effect.

The following two models were used to test for propellant effects:

$$TS = \alpha_0 + \alpha_1 D + \alpha_2 T + \alpha_{1,1} D^2 + \alpha_{1,2} DT + \alpha_{2,2} T^2 \ , \tag{2}$$

and

$$\ln(TS) = \beta_0 + \beta_1 \ln(D) + \beta_2 \frac{1}{K} + \beta_{1,1} [\ln(D)]^2 + \beta_{1,2} \ln(D) \frac{1}{K} + \beta_{2,2} \left(\frac{1}{K}\right)^2 \tag{3}$$

where,

TS	=	Expected tensile strength (lbs/in),
ln(TS)	=	Expected logarithm (base e) of tensile strength,
D	=	Days of exposure to JA-2 vapors,
T	=	Temperature (centigrade) during exposure,
ln(D)	=	Logarithm of days,
K	=	Kelvin temperature (K = T + 273.15), and
α's, β's	=	Coefficients to be estimated by linear regression.

The F-statistics were calculated to be F(6,30) = 0.49 and F(6,30) = 1.49 with 6 and 30 degrees of freedom for model 1 and model 2, respectively. These F-statistic values show the propellant effect is negligible on the estimated model coefficients because the 5% significance level for the F-distribution is F(6,30,0.05) = 2.42.

The data also were examined for each exposure temperature. For each temperature, lines [i.e., $TS = \alpha_0 + \alpha_1 D$, or $\ln(TS) = \beta_0 + \beta_1 \ln(D)$] were fitted to the data with and without propellant. Table 2.10 shows the estimated coefficients and the probability that the coefficients are equal for with and without propellant data. Only one case at 85° C [e.g., $Pr(\beta_{1W} = \beta_{1W/O}) = 0.02$] showed a probability less than 0.05. This result indicates that only at the highest temperature of 85° C did any propellant effect show up in this data set.

Table 2.10. Propellant Effects for Each Exposure Temperature.

Temperature °C	Propellant Effects	Estimated Coefficients α_0	α_1	Estimated Coefficients β_0	β_1
21	Without	331	-0.13	5.73	-0.033
	With	290	-0.35	6.12	-0.114
	Probability	0.07	0.09	0.13	0.18
50	Without	239	-0.17	5.60	-0.057
	With	251	-0.11	5.67	-0.053
	Probability	0.66	0.70	0.78	0.95
70	Without	214	-0.40	5.686	-0.176
	With	202	-0.47	5.857	-0.276
	Probability	0.65	0.66	0.52	0.18
85	Without	223	-3.01	5.615	-0.199
	With	245	-5.94	5.955	-0.444
	Probability	0.67	0.35	0.09	0.02

2.5 Tests of Industrial Pollutants Effects

The variables of temperature and humidity are important external factors in case wall and adhesive joint deterioration. Other external factors which could be important are industrial pollutants to which the rounds may be exposed during storage or deployment. One of the tasks of this program was to survey the literature for potential effects of air pollutants on the component materials of the M829 round. Based on a survey of air pollutant concentrations in the US and Europe, the report (6) recommended that 4-month studies be made of the effects of sulfur dioxide at 0.12 ppm, nitrogen dioxide at 0.11 ppm, and ozone at 0.10 ppm. Because of project delays caused by reviews and documentation required by the National Environmental Policy Act, the exposure period was shortened, and higher concentrations of sulfur dioxide and nitrogen dioxide were used to compensate for the shorter exposures. Ozone was not tested.

The coupons and M919 penetrators were contained in one foot cubed chambers constructed from 1 inch thick Lexan (polycarbonate). These boxes were designed and constructed to meet safety requirements for handling the cellulose nitrate coupons that are considered as explosives. Standards of 100 ppm concentration standards were diluted at the entrance to each chamber to 0.3 ppm NO_2 and 0.5 ppm SO_2 with dry air. Flow of the gas standards and the dilution air were controlled and monitored using ball type rotameters with needle valve controls. NO_2 was monitored using a Rosemount/Beckman model 951A NO/NO_x Chemiluminescence Analyzer. SO_2 was monitored with a National Draeger Ecolyzer. Normally, rotameters and cylinder pressures were checked daily, with weekly

instrument measurement of the NO_2 and SO_2 concentrations. Concentrations were measured at the inlet to the chamber and also within the chamber after mixing. Both SO_2 and NO_2 measurements within the chamber were considerably below the inlet measurements. This is thought to be caused by wall loses of the two components. Both are highly reactive upon dilution.

The exposures continued for 8 weeks at the above stated concentrations with no adverse effects observed in hardness and tensile strength at the end of 2 weeks, 4 weeks and 8 weeks of exposure. To reveal potential effects more clearly, the exposures were made more severe for the remaining month. The concentrations of the two gases were increased to nearly 2 ppm and the exposures were continued. A new set of coupons was inserted in the chambers as comparators with the samples exposed to both the lower concentrations and the new higher concentrations.

Table 2.11 summarizes the exposure conditions and subsequent physical test results. After ca. 8 weeks of exposures at 0.3 - 0.5 ppm, there were no changes in the indentation hardness or tensile strength of the adhesive joint. Therefore, the concentrations were increased to nearly 2 ppm, and the exposures were continued for the last 4 weeks of the study. An additional set of coupons was added to the exposures to test for effects arising from the later, more concentrated exposure, and no effects were detected. There were no significant effects on the coupons from the equivalent of 4 years of exposure to an annual ambient concentration of 0.05 ppm of nitrogen dioxide or to 6 years equivalent exposure to 0.05 ppm of sulfur dioxide. These concentrations represent "worst case" urban pollution. It was concluded that neither of these pollutants in the dry state are important to case wall or adhesive joint deterioration. However, their hydrated forms (acids) may well be damaging. We noted serious effects from nitric acid vapors.

Table 2.11. Effects of Sulfur Dioxide and Nitrogen Dioxide Exposures. (Avg. ± Std. Dev. for n = 4)

Pollutant	Chamber Concentration, ppm	Length of Exposure, Days	Equivalent Ambient Exposure, Years[1]	Ind. Hardness, D-scale		Tensile Strength, lbs/in
				Initial	Final	
NO_2	0.3	16	0.26	68 ± 2.1	66 ± 5.1	206 ± 25.5
	0.3	28	0.46	69 ± 2.3	71 ± 2.3	221 ± 26.5
	0.3	56	0.92	69 ± 2.3	70 ± 2.5	202 ± 7.93
	0.3	64	4.0	69 ± 2.3	69 ± 2.3	197 ± 4.79
	1.6	34				
	1.6	31	2.7	73 ± 2.6	71 ± 2.3	226 ± 57.6
Control[2]	-[3]	-	-	-	68 ± 2.6	172
Control[4]	-[3]	-	-	-	72 ± 2.5	241 ± 40.7
SO_2	0.5	16	0.44	71 ± 2.0	67 ± 5.3	169 ± 15.6
	0.5	28	0.77	71 ± 1.9	72 ± 2.2	241 ± 26.8
	0.5	58	1.6	71 ± 1.9	73 ± 2.6	261 ± 24.3
	0.5	94	6.1	73 ± 1.8	74 ± 3.3	283 ± 49.4
	1.9	34				
	1.9	31	3.2	73 ± 2.2	74 ± 1.9	220 ± 29.2
Control[5]	-[3]	-	-	-	71 ± 3.0	246
Control[4]	-[3]	-	-	-	72 ± 2.5	241 ± 40.7

[1]Equivalent exposure in years at annual ambient average of 0.05 ppm for each of SO_2 and NO_2.
[2]Control (n = 1) for 0.3 ppm NO_2 tests.
[3]Controls stored in explosives magazine.
[4]Controls (n = 8) for 1.6 ppm NO_2 and 1.9 ppm SO_2 tests.
[5]Control (n = 1) for 0.5 ppm SO_2 tests.

3. ACCELERATED ENVIRONMENTAL EXPOSURE OF FULL-UP M829 ROUNDS AND DEVELOPMENT OF PREDICTIVE MODELS

Mathematical models of the skive joint behavior in response to external environmental stresses are needed to predict useful field lifetimes of the M829 and to identify limits for storage conditions. This chapter reports the findings from the statistically designed accelerated environmental exposure study of full-up M829 rounds.

3.1 Accelerated Environmental Exposure Experiment

Full-up M829 rounds for this study were manufactured in December, 1989, to military specifications on the Milan Army Ammunition Plant (MAAP) M829 production line, using calibration hardware provided by the Iowa Army Ammunition Plant. The sequentially numbered rounds were kept in standard metal protective cases and stored in a bunker until use. The accelerated environmental exposures were conducted in temperature-and humidity-controlled chambers housed in a remote area of the MAAP. After each exposure experiment, the rounds received a battery of tests: a visual inspection of the case wall and coating condition, chambering test on the production line chamber gauge, diameter measurement at the skive joint to test for swelling, measurement of the case wall indentation hardness (D-scale durometer) at several points located around the circumference of the round at the skive joint and midway down the round as well as at intermediate points down the side of the case, and determination of the tensile strength of the skive joint using a Slota apparatus. Indentation hardness measurements around the adapter base were added after the start of the study.

Time, temperature, and humidity are three environmental factors most likely to affect the deterioration of skive joints. Tensile strengths were measured on skive joints for full-up M829 rounds subjected to different combinations of these environmental factors. From these experiments, a mathematical model was developed to predict the tensile strength of the skive joint as a function of the environmental factors. Initial examination of previous studies by AMCCOM and Honeywell (1-3) suggested that a second-order polynomial was required to predict tensile strengths. A central-composite experimental design (5) was employed to estimate both first-order and second-order coefficients. Table 3.1 gives the levels of the three environmental factors in the central composite design. Figure 3.1 illustrates the three components of central composite designs: factorial or cube points $(\pm1,\pm1,\pm1)$ NF = 8; axial points $[(\pm a,0,0),(0,\pm a,0,),(0,0,\pm a)]$ NA = 6; and center points (0,0,0) NC = 4. The exposure ranges selected for this experiment included those temperatures used in previous AMCCOM and Honeywell studies (1-3). Also, the temperatures and humidities overlapped those measured in the M1A1 hull and bustle ammunition compartments (7) in continental US and European deployment, as well as those reported for shipboard prepositioned storage and Middle East storage areas (8). The highest temperatures actually extended beyond those found in the field to shorten the time required for observation of exposure effects.

Table 3.1. Levels of the Environmental Factors for the Central Composite Design.

	Levels				
Factors	-a	-1	0	+1	+a
Time (weeks)	2	6	12	18	22
Temperature (°C)	40	50	60	70	80
Humidity (% relative)	25	40	60	80	95

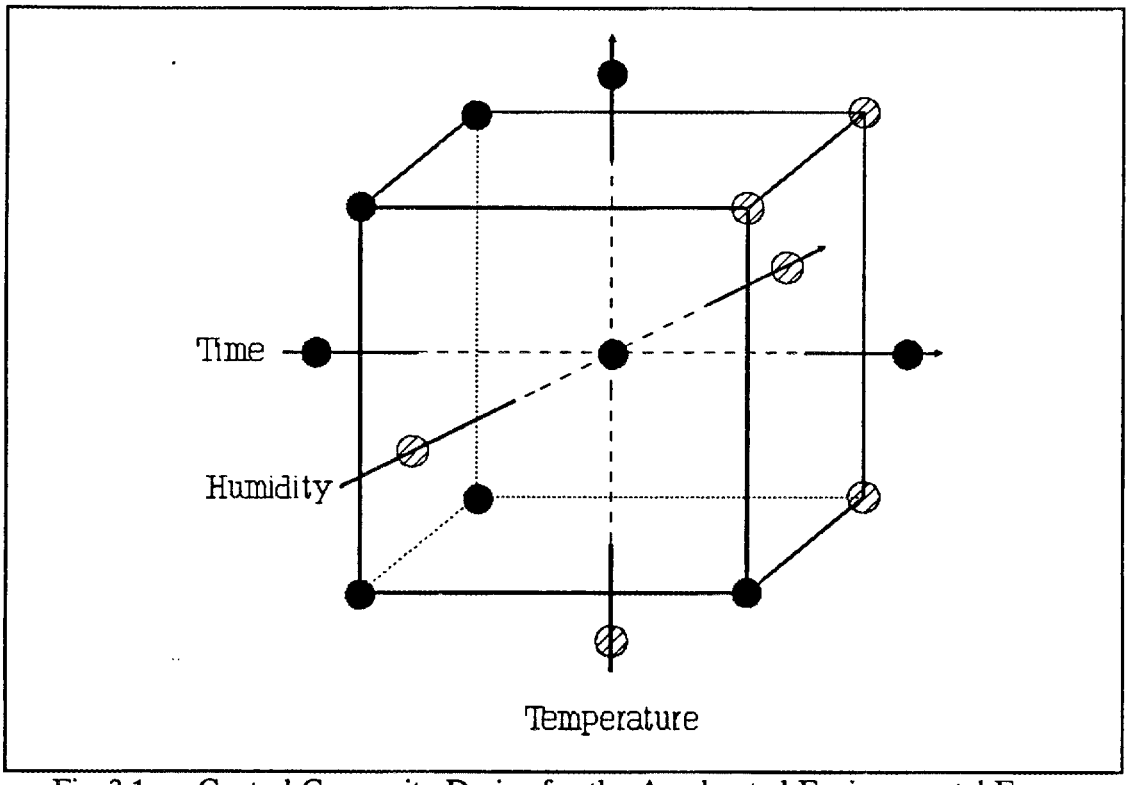

Fig. 3.1. Central Composite Design for the Accelerated Environmental Exposures of M829 Rounds. (Solid circles are completed experiments. Shaded circles are uncompleted experiments.)

Simultaneous with the accelerated environmental exposure experiment, M829 rounds also were removed from bunker storage and subjected to the same battery of tests as those in the central composite design. These M829 rounds served as controls. The control rounds

also should show effects of storage under conditions similar to parts of western Europe. At each condition in the accelerated environmental exposure experiment, four replicate M829 rounds were run except for two ambient tests of one-week and eight-weeks durations. These two ambient tests had seven and three replicates, respectively. All M829 rounds were assigned randomly to the environmental exposure conditions.

3.2 Results of Accelerated Environmental Exposures

The appearance of the M829 case wall changed considerably during some of the severe exposures. Figure 3.2 shows combustible case wall sections taken from just below the skive joint after the tensile strength testing was conducted. For the 85°C exposures, the case wall coating turned a golden brown after 2 weeks of exposure, and to a reddish brown after 3 weeks. The nitrocellulose also turned to an orange-brown color. This discoloration is probably from the accumulation of nitrated diphenylamines derived from the Akradite II stabilizer. Considerable case wall softening accompanied the color changes. The importance of humidity in case wall deterioration also is evident from the appearance of the specimens shown for 70°C exposures at 40 and 80% RH.

The figure also shows that the disbonding observed at 85° was a "clean" adhesive failure. A cohesive mode of failure in the nitrocellulose immediately below the adhesive was observed in all tensile strength tests where a finite strength was determined.

Table 3.2 lists tensile strength data from the truncated (i.e., experiment terminated in June 1991) accelerated environmental exposure experiment. These data were used to develop the tensile strength prediction model for the M829 skive joint tensile strength.

Fig. 3.2 M829 Case Wall Sections Taken just below the Skive Joint after Accelerated Environmental Testing.

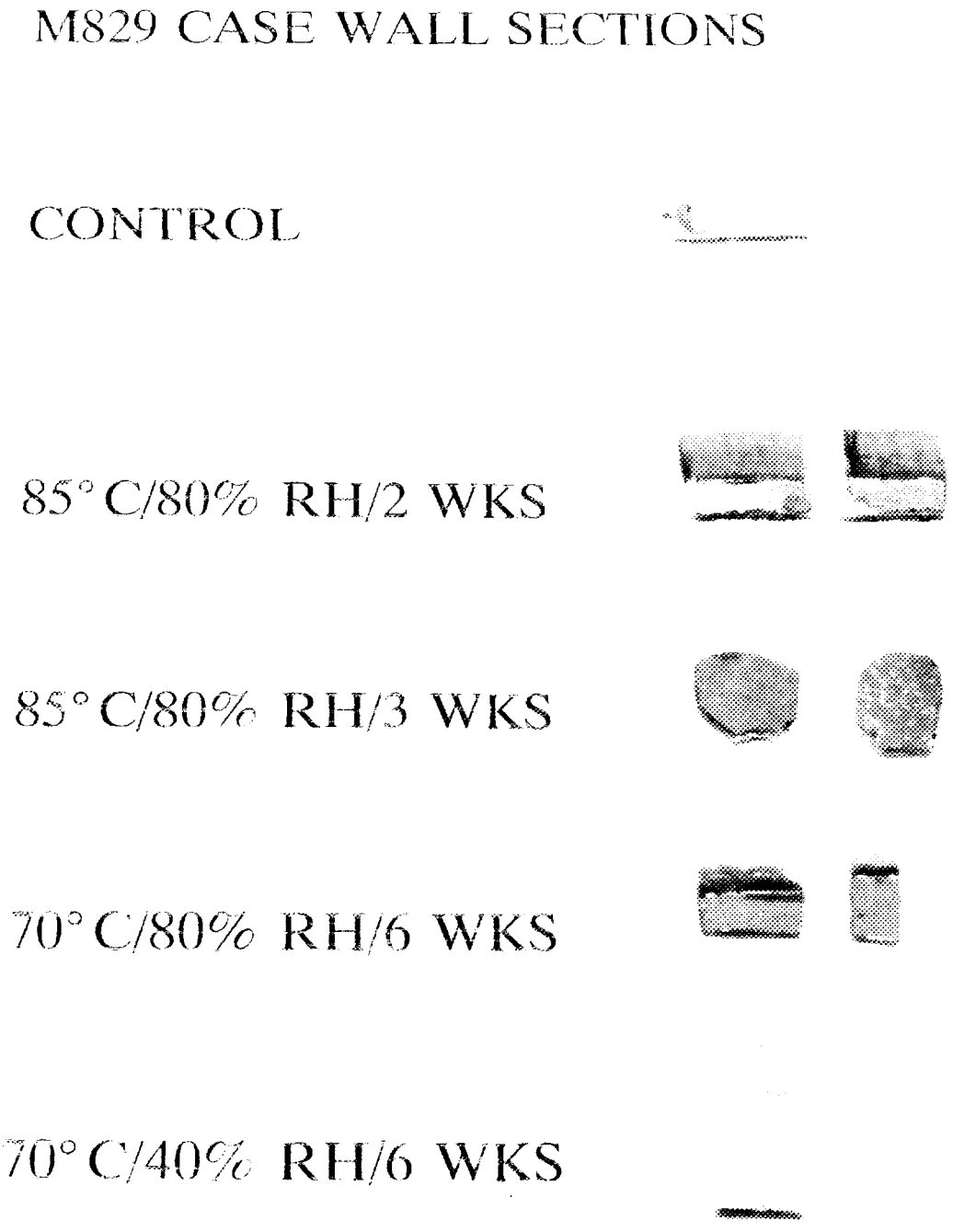

Table 3.2. Tensile Strength Data from the Accelerated Environmental Exposure Experiment.

Run	Weeks	Temperature (°C)	Relative Humidity (% RH)	Tensile Strength (lbs)	Average (lbs)	Standard Deviation (lbs)	Design Type
1-3	1	9	74	2972,3082,3269,3851, 4110,4146,4683	3730	639	Ambient
2-2	2	60	60	3675,3775,3851,4115	3854	188	Axial
3-1	2	70	80	1286,1828,3601,4154	2717	1377	Test
4-2	2	85	80	0,0,0,0	0	0	Test
5-2	3	85	80	0,0,0,0	0	0	Test
6-2	6	50	40	1556,3473,3802,4665	3374	1312	Cube
7-1	6	50	80	1315,2118,3156,4123	2678	1223	Cube
8-1	6	70	40	1120,1207,2612,2947	1972	944	Cube
9-2	6	70	80	0,0,0,0	0	0	Cube
10-3	8	9	74	2574,2624,3352	2850	436	Ambient
11-2	12	60	60	2199,2767,2837,3001	2701	349	Center
12-2	12	80	60	0,0,0,0	0	0	Axial
13-1	18	50	40	227,944,1895,2336	1351	948	Cube
14[a]	18	70	80	0,0,0,0	0	0	Cube
15-2	22	60	60	0,0,0,0	0	0	Axial
16-3	43	15	71	3082,3435,3563,3646	3432	249	Ambient
17-3	49	15	71	3226,3604,3779,4112	3680	369	Ambient

[a] Results based on tensile strength values of run 9-2.
Note: Second number of Run denotes test chamber (i.e., chamber 1, chamber 2, and storage bunker 3).

Replicate tensile strengths measured on 6 of the 17 experimental design points were zero (i.e., the joints disbonded in the test chamber). From the non-zero values, an estimate of tensile strength variation was obtained by pooling the standard deviations (S_{rep}) of the replicate measurements. This estimated pooled standard deviation had 35 degrees of freedom:

$$S_p = 838.$$

This estimate of tensile strength variation is independent of any mathematical model used to predict tensile strengths. The variation due to replicate measurements also implies an upper bound on the amount of total variation from the average that can be explained by any prediction model.

3.3 Predictive Models of Skive Joint Tensile Strength

Polynomial models were initially used to predict skive joint tensile strengths. This standard approach assumed that the true underlying theoretical function can be approximated by a truncated Taylor's series expansion. First-order and second-order terms of the experimental factors (i.e., time, temperature, and relative humidity) were candidates to be included in the approximating polynomial. Approximating polynomial models accounted for the variability of tensile strength values reasonably well in the experimental region defined by the data. However, extrapolating tensile strength values outside the experimental region was found to be completely misleading. For example, predicted values from polynomial models indicated that tensile strength would increase with time. For skive joint disbonding (zero tensile strength values), predicted values were negative. Alternative tensile strength models were investigated to overcome the prediction deficiencies of the approximating polynomial model.

Figure 3.3 shows the data plotted as increasing average tensile strength versus the experimental conditions. This plot shows the tensile strength (TS) data is either at a low level (e.g., TS = 0 lbs) or at a high level (e.g., TS $\geq$ 2500 lbs). Only two experimental conditions show average tensile strength between these two values (e.g., 1350 lbs $\leq$ TS $\leq$ 2000 lbs). Figure 3.3 also shows the large variability in skive joint strength that was observed for each of the exposures.

Several models (including Arrhenius and kinetics models) based on nonlinear growth (9,10) were investigated that would predict positive near-zero values for conditions resulting in

joint failure (zero tensile strengths). In addition, predicted tensile strength should start at a limiting value at ambient conditions. The logistic model has these two properties and gives consistent extrapolation results. The form of the logistic model is:

$$TS = \frac{A}{[1 + \exp(B + C_1 t + C_2 T + C_3 H + C_4 T*H)]} + \epsilon .$$

where TS = tensile strength (lbs), t = time (weeks), T = temperature (°C), and H = relative humidity (%RH). The coefficients (i.e., A, B, C_1, C_2, C_3 and C_4) were estimated from the data in Table 3.2. The ϵ represents the measurement error. The logistic model has an S-shape curve for any one of the independent variables.

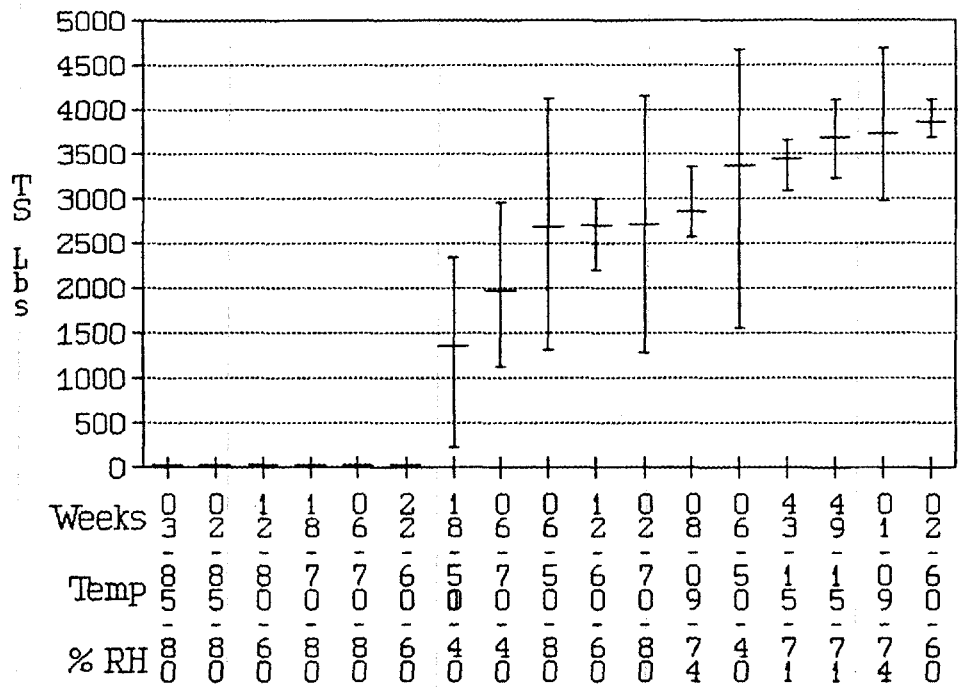

Fig. 3.3. Tensile Strength Data Ordered by Increasing Average Value.

As the independent variables increase [e.g., (t,T,H) → ∞], the tensile strength approaches zero. As the independent variables decrease [e.g., (t,T,H) → -∞], the tensile strength approaches the limiting value of TS = A. This logistic model represents the change in tensile strength with respect to any one of the three independent variables (i.e., dTS/dX_j,

where X_1 = t, X_2 = T, and X_3 = H) to be proportional to the product of the present tensile strength (TS) and the future tensile strength (A - TS):

$$\frac{dTS}{dX_j} = \frac{-C_j\ TS\ (A - TS)}{A} \qquad j = 1,\ 2,\ 3.$$

The coefficients in the logistic model were estimated by nonlinear regression (5,9) using Marquardt's procedure (11). Four outlier values were identified by the initial fitting of the data. These unusual tensile strength values were more than 2.5 standard deviations from the predicted values (i.e., 1286 lbs, 4154 lbs in Run 3-1; 1556 lbs in Run 6-2; and 1315 lbs in Run 7-1). We set aside these outlier values to develop the logistic model. The refitted logistic model accounted for 91% (the maximum value is 93%) of the total variation of measured tensile strengths from the average. In addition, no significant lack of fit could be detected at the 5% significance level when the variance estimated by the logistic model was compared with the variance estimated from replicate measurements. The estimated coefficients with 95% confidence intervals are given in Table 3.3. An example of the logistic model response surface is given in Figure 3.4.

Table 3.3. Logistic Model Coefficients Estimated by Non-linear Least Squares.

Parameter	Estimate	Standard Deviation	Lower 95% Confidence Interval	Upper 95% Confidence Interval
A	3566.479	99.362	3367.793	3765.164
B	-42.081	(a)	(a)	(a)
C_1 (weeks)	2.439	0.319	1.802	3.076
C_2 (°C)	0.267	0.051	0.166	0.368
C_4 (% RH)	-1.818	0.370	-2.559	-1.077
C_3 (°C*%RH)	0.029	0.006	0.017	0.041

(a) The variance of B could not be estimated from the truncated accelerated environmental exposure experiment.

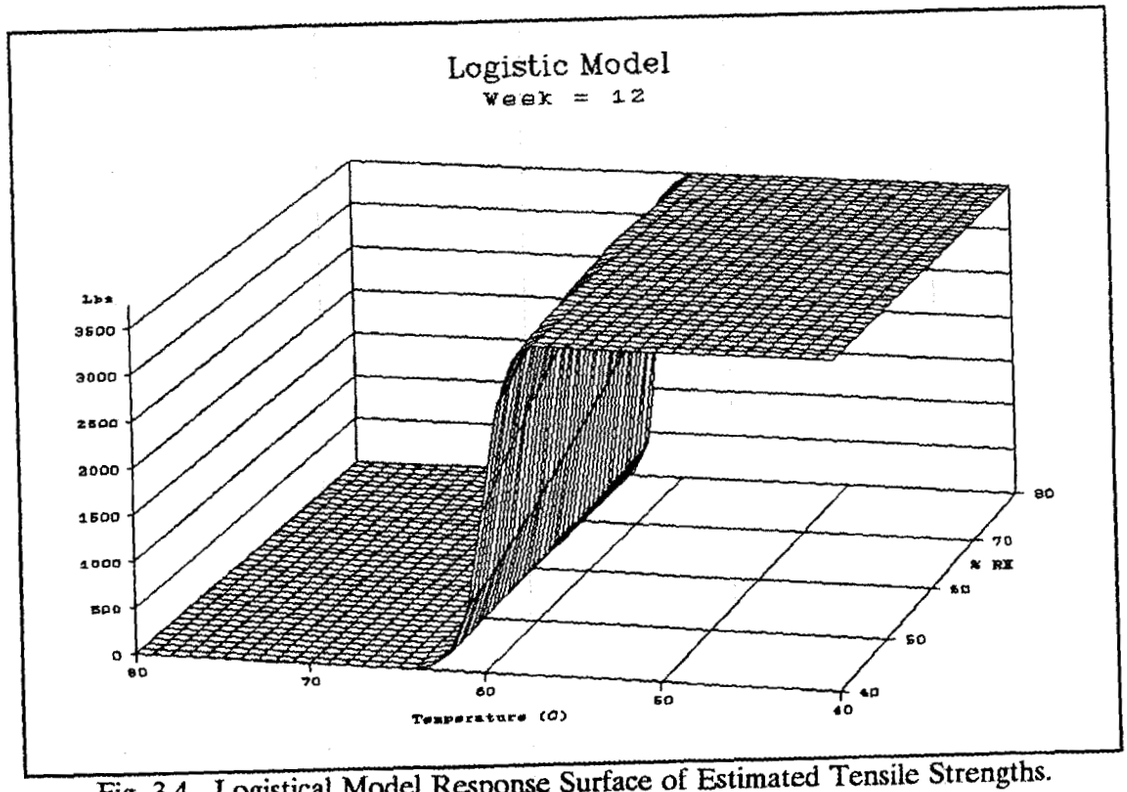

Fig. 3.4. Logistical Model Response Surface of Estimated Tensile Strengths.

Figures 3.5, 3.6, and 3.7 give prediction values and the two sided 95% confidence intervals for three conditions (21°C, 80% RH), (35°C, 50% RH), and (66°C, 90% RH), which include worst case conditions for Operation Desert Storm. Logistic predictions for these cases are all less than 52 weeks. These prediction values seem unusually short in view of actual field experience. The upper 95% confidence interval reached an asymptotic limit of 1051 lbs at the time point the average tensile strength was predicted to be zero. Therefore, the short time predicted for skive joint deterioration and failure is the time beyond which a round could have any tensile strength in the interval $0 \leq TS \leq 1051$ lbs. This wide interval again reflects the large variability in round-to-round strength.

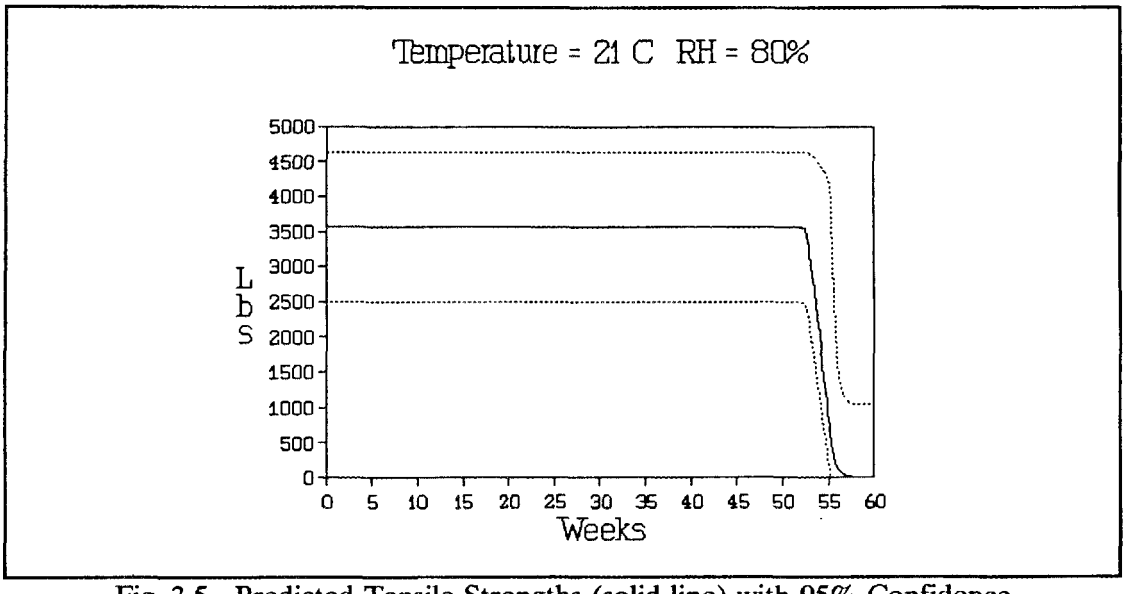

Fig. 3.5. Predicted Tensile Strengths (solid line) with 95% Confidence Intervals (dotted lines) for Exposure at 21°C and 80% RH.

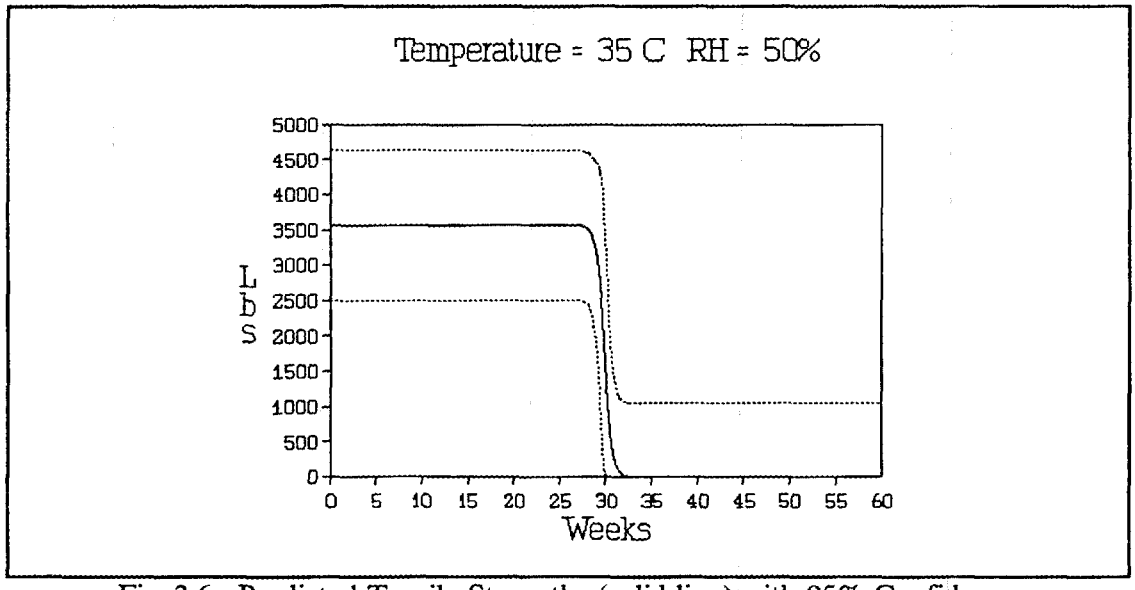

Fig. 3.6. Predicted Tensile Strengths (solid line) with 95% Confidence Intervals (dotted lines) for Exposure at 35°C and 50% RH.

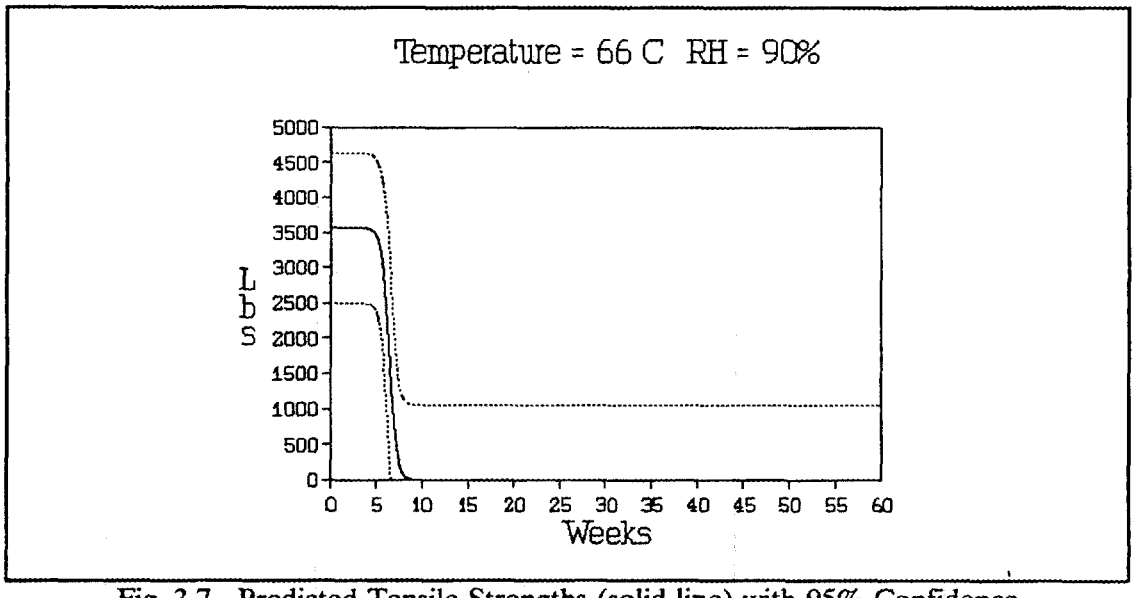

Fig. 3.7. Predicted Tensile Strengths (solid line) with 95% Confidence Intervals (dotted lines) for Exposure at 66°C and 90% RH.

At the suggestion of Dr. Eric Bixon of AMCCOM, a kinetic model also was evaluated. This model was constructed as described below:

1. Fit zero-order models (e.g. lines) to the degradation of tensile strength versus time for a series of fixed temperatures. The relative humidities were in the range 60-80% and were assumed to have no effect.

$$\frac{d(TS)}{dt} = -K \ . \quad \textit{Temperature fixed.}$$

or

$$TS_0 - TS = Kt \ . \quad \textit{Temperature fixed.}$$

where,

TS	= tensile strength at time t.
TS_0	= tensile strength at time t=0.
K	= zero-order rate constant in units of (lbs/week).

2. Fit an Arrhenius Model to the rate constants (e.g. K's). Use this prediction equation to estimate rate constants at lower temperatures.

$$K = K_0 \exp(-E/RT) \ .$$

or

$$\ln(K) = A + B\left(\frac{1}{T}\right) .$$

where,

A,B	= intercept and slope to be estimated by the method of least squares.
T	= absolute temperature T = °C + 273.15.

The estimated rate constants were based on selected values from the response surface experiment. Table 3.4 lists the data values from this experiment.

Table 3.4. Tensile Strength Data Used to Estimate Rate Constants.

Temperature (°C)	Time (weeks)	Tensile Strength (lbs)	Average (lbs)	%RH
Ambient	1	2972,2851,4110,4146 3082,3269,4683	3730	Ambient
50	6	1315,2118,3156,4123	2678	80
60	2	3675,3775,3851,4115	3854	60
	12	2199,2767,2837,3001	2701	60
70	2	1286,1828,3601,4150	2717	80
	6	0,0,0,0	0	80

The average tensile strength for ambient bunker storage at week t = 1 was an estimate of the tensile strength at time t = 0 (e.g, TS_0 = 3730). The tensile strength at failure was taken as 200 lbs. This value is the nominal value for the lowest real tensile strength observed in the response surface experiment (e.g. 227 lbs). Estimated lifetimes were calculated by:

$$Lifetime\ (weeks) = \frac{(3730-200)\,lbs}{RateConstant\,(lbs/week)}\ .$$

Estimated rate constants were calculated by linear regressions of (TS_0 - TS) versus time for each temperature. The linear regressions go through the origin at time t = 0 to indicate the starting tensile strength is TS_0. Rate constants were the slopes estimated from this regression. Table 3.5 lists the slopes for each of the three temperatures. Figure 3.8 plots the results of the linear regression.

Table 3.5. Rate Constants Estimated from the Linear Regression of (TS_0 - TS) = Kt.

Temperature (°C)	Rate Constant (lbs/week)	Standard Deviation (lbs/week)
50	175.3	101.9
60	81.8	14.0
70	610.1	72.4

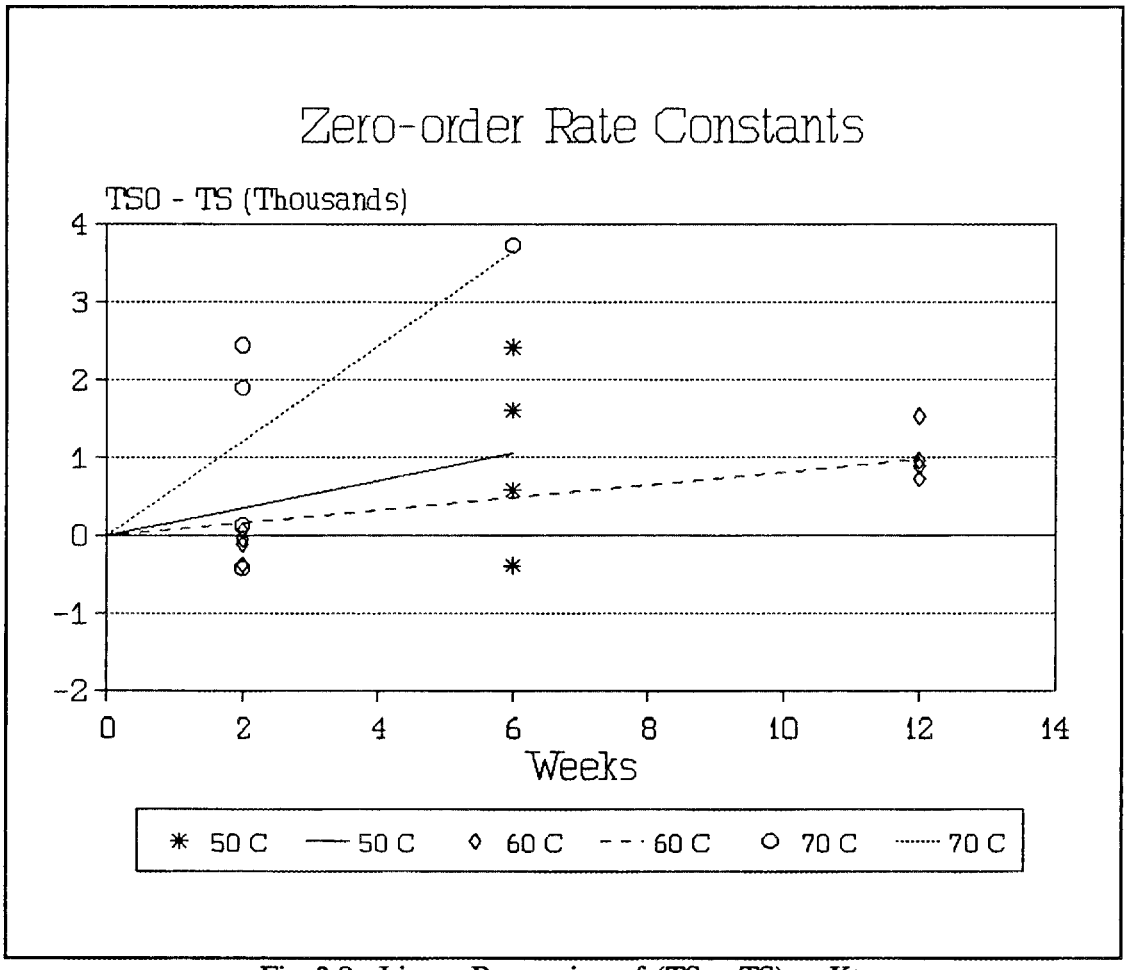

Fig. 3.8. Linear Regression of (TS_0 - TS) vs Kt.

Rate constants were estimated by an Arrhenius Model for temperatures other than 50°C, 60°C, and 70°C. The logarithm (base e) of the rate constants estimated in Table 3.5 were regressed on the inverse of the absolute temperatures [e.g., 1/(°C + 273.15)]. This Arrhenius line can predict rate constants for different temperatures. The Arrhenius prediction line with coefficient standard deviations in parentheses is given by:

$$\ln(K) = \underset{(27.02)}{25.63} - \underset{(8993.33)}{6758.05}\,(1/T) \; .$$

Figure 3.9 Shows an Arrhenius plot and Table 3.6 gives estimated rate constants and lifetimes for the temperature range 20°C to 80°C.

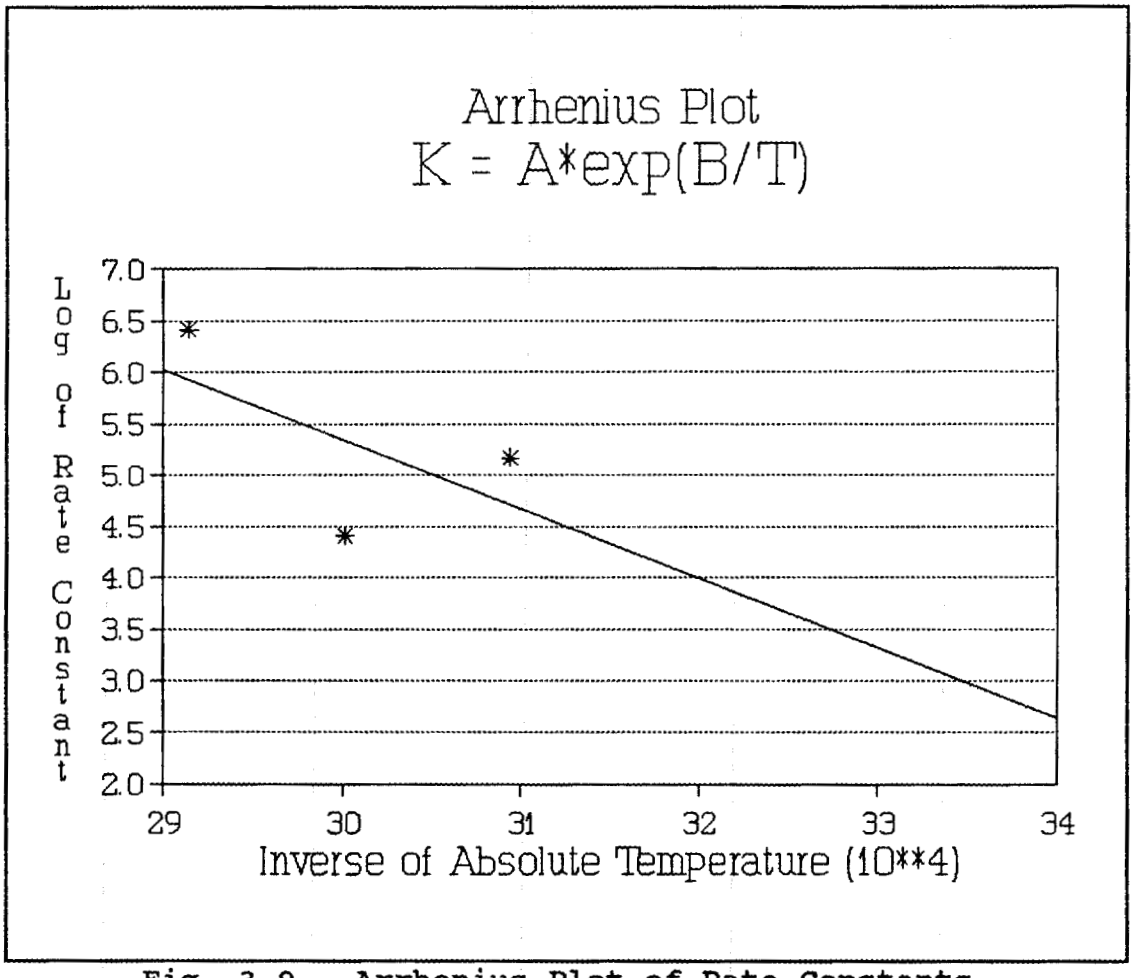

Fig. 3.9. Arrhenius Plot of Rate Constants.

Table 3.6. Estimated Rate Constants and Lifetimes for Temperatures 20°C to 80°C.

Temperature (°C)	Rate Constant (lbs/week)	Lifetime (weeks)
20	13.096	270
25	19.277	183
30	28.016	126
35	40.226	88
40	57.092	62
45	80.145	44
50	111.330	32
55	153.109	23
60	208.562	17
65	281.514	13
70	376.676	9
75	499.809	7
80	657.903	5

The temperature-dependence of the skive joint lifetime is evident in the predictions shown in Table 3.6. A small 5°C increase in temperature, from 20° to 25°C, is predicted to decrease the lifetime from 5.2 years (270 weeks) to 3.5 years (183 weeks). This suggests a highly temperature-dependent deterioration mechanism in the M829 skive joint.

These predictions must be considered as tentative because of the large round-to-round variability and the resulting scatter in the data points used to fit prediction equations, and the large confidence intervals about the plots. On the other hand, considering these uncertainties, the lifetime prediction of 5.2 years at 20°C is in good agreement with the 4.8 years prediction based upon nitroester migration rates in the AMCCOM study (2). This agreement suggests the utility of the kinetic modelling approach in the predictive surveillance of this munition component.

3.4 Comparison with Tensile Strength Data from Lot Acceptance Testing

The sources of the round-to-round variability, which limits the precision of predictive models, should be determined to allow engineering which could improve the uniformity of the skive joint. One type of data which can be useful is from lot acceptance testing conducted on the same equipment by the same protocols as for the full-up rounds. Tensile strength data from lot acceptance tests (but not for the same lots as the M829s

used in this study), supplied by MAAP (12), consisted of pull-tests on M829 adaptor/case surrogate assemblies (not full-up rounds). Tensile strengths were recorded on 157 unloaded assemblies from four production lots. All pull-tests were made within a maximum of 2 days after fabrication.

Pull-tests for lot acceptance tests were made on 157 adaptor/case assemblies from 4 production lots. At the MAAP, production lot numbers are changed if a major component (e.g., propellant) changed, or the fabrication of M829 rounds stopped for 48-72 hours. The data were collected in May, June, July, and August of 1989. The ranges for temperature and relative humidity during adhesive joint curing were 20°C to 37°C and 33% to 92%, respectively. A statistical analysis could not detect any effects on tensile strength measurements due to temperature or relative humidity during adhesive curing.

This result is not surprising because the pull-tests were made shortly after fabrication and the period of environmental exposure was relatively short. A histogram is given in Figure 3.10 for the tensile strength measurements for the production data. Summary statistics are listed in Table 3.7 for each lot.

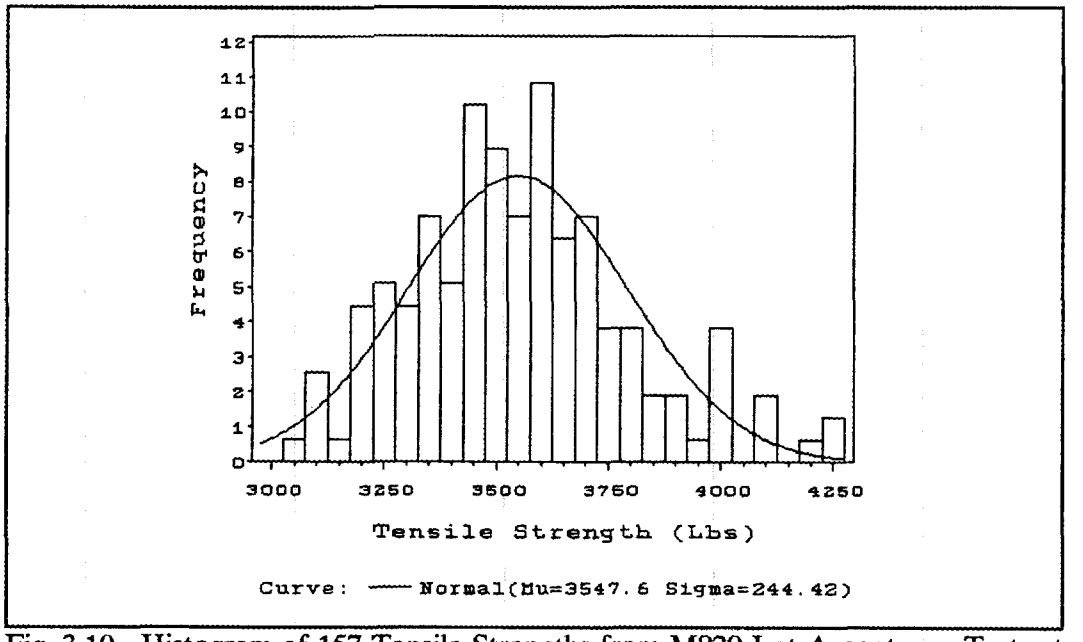

Fig. 3.10. Histogram of 157 Tensile Strengths from M829 Lot Acceptance Tests at the MAAP.

The histogram shows an average tensile strength of TS = 3548 with a standard deviation of S_M = 244. The superimposed normal distribution indicates the tensile strengths were not normally distributed and were skewed to the lower tensile strength values.

Table 3.7. Tensile Strength (lbs) Summary Statistics for MAAP Lot Acceptance Tests.

Production Lot	Number	Average Tensile Strength	Standard Deviation	Range
1	33	3607	271	3078-4226
2	41	3472	151	3224-3849
3	31	3502	244	3183-4251
4	52	3596	271	3030-4177
Total	157	3548	244	3030-4251

The tensile strengths for the four production lots are plotted as box plots on a quality control chart in Figure 3.11. The box plot for each lot shows the maximum, 75th percentile, median (horizontal line), mean (+), 25th percentile, and minimum. The box contains the middle 50% of the data from the 25th percentile to the 75th percentile. The quality control chart puts upper and lower 3-sigma limits on the average tensile strength of each production lot. Figure 3.10 shows that the average tensile strengths for the production lots were all within the control limits.

The average tensile strengths from MAAP lot acceptance tests and the full-up M829 rounds stored under ambient bunker conditions were not significantly different. But, the standard deviation of tensile strength measurements for the full-up M829 rounds was four times as large as the standard deviation of tensile strength measurements for the M829 case/adaptor assemblies. Initially, nitroester diffusion was considered the cause for the increased variation. This cause was rejected after a preliminary analysis of case wall samples from several full-up M829 rounds indicated little or no nitroester migration (see section 3.6). The increased variation of full-up M829 rounds versus adaptor/case assemblies most likely is due to the additional fabrications steps required for production of the full-up M829 rounds. The ambient tensile strength data also suggest that lot acceptance tests cannot measure round-to-round variability in the full-up M829 rounds.

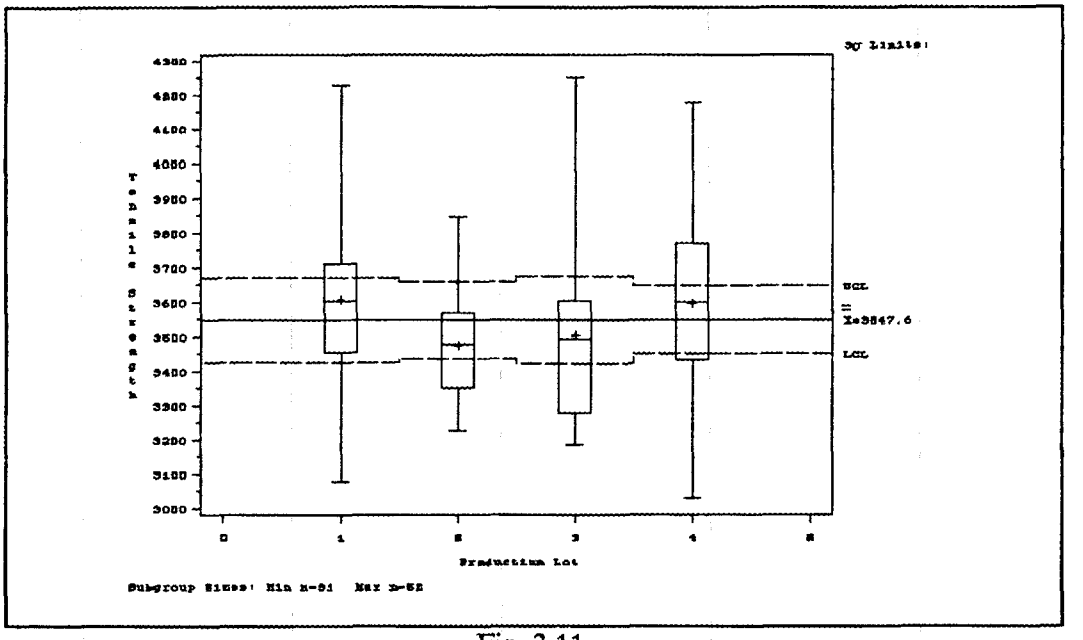

Fig. 3.11.

Box Plots and Quality Control Chart for MAAP Lot Acceptance Tests.

3.5 M829 Case Wall Indentation Hardness

As noted in section 3.1, other properties of the rounds were measured after the accelerated environmental exposures. These consisted of the diameter of the skive joint (measure with a calipers), case wall hardness (D-scale durometer), and chambering test (production line chamber gauge). Case wall swelling was not detected in any exposure, and all rounds which did not disbond in the exposure chamber passed the chambering test. These data are not reported. In only a few cases was the indentation hardness of the case wall affected. These data are listed in Table 3.8, along with the ranges of values for the bunker storage control rounds.

Table 3.8. Case Wall Indentation Hardness for Selected Accelerated Environmental Exposures. (Avg. ± Std. Dev. for n = 4, except for ranges observed with bunker controls)

Experiment	Time, Weeks	Temp., °C	RH, %	Indentation Hardness (D-scale)		
				Mid.	Joint	Adapter
2-1	2	85	80	54 ± 1.7	54 ± 1.7	53 ± 2.3
2-2	3	85	80	46 ± 4.4	41 ± 2.4	-
2-3	6	70	80	24 ± 5.7	24 ± 4.5	-
Range for Controls	-	-	-	68 - 75	59 - 75	76

Very little case wall softening effects were observed from the exposures, and the Table 3.8 contains data for only those exposures where effects were observed. These were for the two highest temperatures and highest relative humidities, so it was not surprising that softening occurred. Case wall softening appeared to be approximately equal along the length of the case wall from the adapter to the middle section of the combustible cartridge case. The cellulosic adapter did not soften more than the nitrocellulose under these conditions. The lack of effects after other severe exposures which caused disbonding was not expected. This observation suggests that the case indentation hardness is a more "robust" property than the tensile strength of the skive joint, and that the latter should be the major concern of predictive surveillance. Proper care of the latter should preserve the former.

3.6 Nitroester Migration into the M829 Case Wall

M829 rounds selected from the accelerated environmental exposure study to represent a wide range of skive joint strengths were characterized for nitroester content to test for a relationship between nitroester migration and skive joint strength. Ca. 1 g samples of the M829 nitrocellulose case wall immediately below the skive joint were analyzed for diethyleneglycol dinitrate (DEGDN), nitroglycerin (NG), and Akardite II (methyldiphenyl urea) by the same procedure as used by Dr. Chen of ARDEC. Briefly, ca. 1 g samples from selected rounds were ultrasonically extracted in methanol, allowed to soak 48 hrs, were re-sonicated, and then the supernatant was diluted and analyzed using high performance liquid chromatography with ultraviolet absorbance detection. Reanalysis of some extracts after an additional 48 hr soaking and resonication did not reveal significantly more nitroesters, suggesting that extraction was complete.

The first samples were analyzed to establish the uniformity of the nitroester and stabilizer distribution around the circumference of the case wall. Four case wall specimens taken 90° apart around the nitrocellulose side of the rim of the skive joint were analyzed for two rounds. The results are listed in Table 3.9. The data suggested that all three constituents were uniformly distributed around the circumference of the round at the skive joint, and that only a single specimen needs to be analyzed. There was a concern that the horizontal position of the rounds during the accelerated environmental exposures would lead to a settling of the propellant more toward the bottom side of the round, and would result in an uneven nitroester migration. Other work at AMCCOM (15) suggests that nitroester migration into the case wall occurs predominantly by capillary action where the propellant contacts the propellant bug and case wall. Thus, propellant settling in these tests must have been minimal.

Case wall samples from selected M829 rounds were then subjected to the analytical method, and the results are presented in Table 3.10. A plot of the total nitroester concentration (DEGDN + NG) versus skive joint tensile strength is shown in Figure 3.12. As in previous work (1-3), there is a rough relationship between nitroester concentration and skive joint strength. A least squares linear regression of the data yielded a correlation coefficient of -0.761. The nitroester concentration corresponding to 0 lbs tensile strength was 153 mg/g, which is considerably higher than the ca 60 mg/g suggested in previous work (2). The nitroester concentration predicted for the lowest tensile strength actually measured in this study, ca. 200 lbs, corresponded to 144 mg/g of nitroesters. The differences between the two studies may reflect the different lots of ammunition, round-to-round variability, and the basic differences in how the exposures were conducted in the two studies.

Clearly, the higher the nitroester concentration, the weaker the skive joint will become. Somewhere in the low weight percent concentrations, the joint will disbond. This suggests that a means of visually indicating the nitroester content of the case wall at the skive joint could allow in-field surveillance of M829 rounds (and other munitions with such adhesive joints) and identification of those liable to failure. Accordingly, a study was made of chemical systems for a color change strip which could visually indicate the presence of nitroesters in the M829 case wall. The results of that survey are reported elsewhere (13).

Table 3.9. Uniformity of Nitroester and Stabilizer Distribution in Nitrocellulose Wall at the Skive Joint.

Round No.	Replicate	Concentration in Case Wall, mg/g		
		Akardite II	DEGDN	NG
108	1	2.72	90.2	60.9
	2	2.59	91.4	63.5
	3	2.57	87.9	59.4
	4	2.45	78.2	54.1
	Avg. ± Std. Dev. (%RSD)	2.58 ± 0.11 (4.3%)	86.9 ± 6.0 (6.9%)	59.5 ± 4.0 (6.7%)
54	1	3.75	97.0	66.4
	2	3.89	102.0	72.4
	3	3.41	94.2	64.4
	4	3.20	86.4	59.6
	Avg. ± Std. Dev. (%RSD)	3.56 ± 0.32 (8.8%)	94.9 ± 6.5 (6.9%)	65.7 ± 5.3 (8.1%)

Table 3.10. Results for Nitroester and Akradite II Measurements in M829 Nitrocellulose Case Wall at the Skive Joint after Accelerated Environmental Exposures.

Test	Round No.	Temp., °C	Humidity, % RH	Time, Weeks	Concentration in Case Wall, mg/g			Tensile Strength, lbs
					Akardite II	DEGDN	NG	
Control	100	-	-	-	5.16	1.81	1.49	4,683
	129	-	-	-	6.54	1.97	ND	3,851
	153	-	-	-	27.5	0.66	0.54	3,269
	63	-	-	-	9.44	2.47	2.26	1,259[1]
	78	-	-	-	21.0	2.45	2.35	4,145
2-1	5	85	80	2	13.4	55.6	60.6	0
	47				2.78	68.3	46.6	0
	65				1.72	73.0	48.2	0
	162				1.66	69.3	47.3	0
1-3	108	40	60	12	2.58	86.9	59.5	0
	148				2.69	91.9	64.2	0
	54				3.56	94.9	65.7	517
	105				3.60	73.7	46.1	2,480
1-2	151	70	40	6	<0.01	19.3	10.5	2,947

	30				1.13	28.8	18.1	1,207
	138				5.79	51.6	27.2	1,120
	37				11.9	48.2	24.2	2,612
1-1	4	50	80	6	3.33	16.2	7.50	4,123
	160				25.0	18.0	8.55	2,118
	161				6.05	16.0	6.75	1,315
	68				4.96	16.2	8.89	3,156
1-5	118	70	80	2	6.35	41.7	23.3	1,286
	39				5.84	34.0	19.0	1,828
	52				2.71	33.2	19.3	3,601
	114				4.70	28.0	8.89	4,154
2-8	67	50	40	6	7.54	24.9	9.22	3,473
	156				16.8	27.6	15.6	3,802
	16				0.01	19.9	9.16	1,556
	115				0.28	13.5	3.92	4,665

[1]Skive joint and case damaged in Slota apparatus fixture. Strength is artificially low.

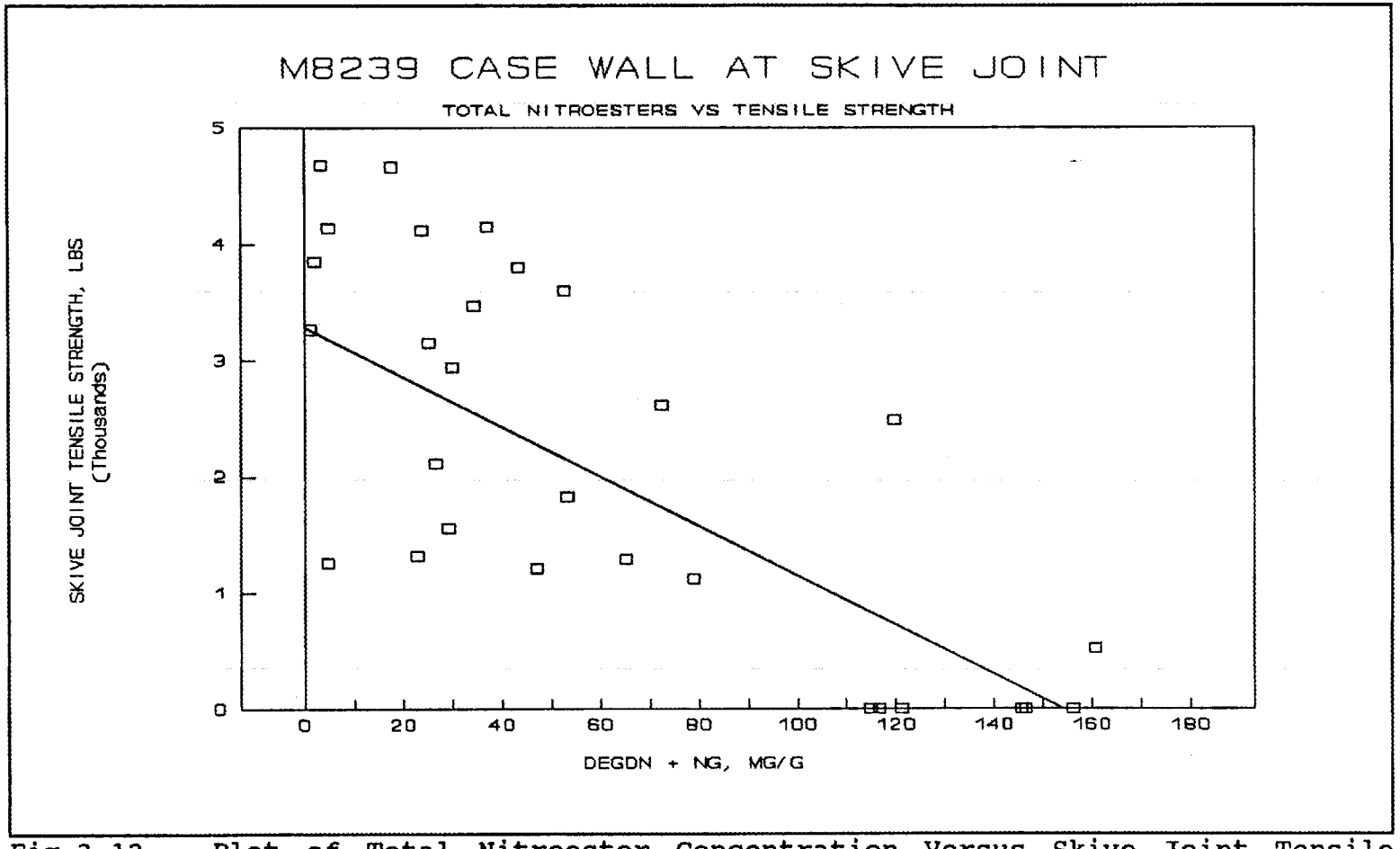

Fig.3.12. Plot of Total Nitroester Concentration Versus Skive Joint Tensile Strength in M829 Rounds from Accelerated Environmental Exposures.

4 CONCLUSIONS AND RECOMMENDATIONS

The laboratory studies with combustible cartridge case coupons have allowed the identification of important factors in case wall and adhesive joint deterioration. The conclusions of this work are,

1. Temperature, as well as humidity, are important external effects, but humidity is important only at higher % RH near saturation. Humidity effects are reversible except at elevated temperatures, where hydrolysis of the nitrocellulose polymer may be significant.

2. Propellant-related internal effects are important under at least two exposure conditions: elevated temperatures and aqueous leaching. The latter corresponds to a round lying in a pool of water. These effects are attributed to nitrogen oxide evolution and nitroester migration (elevated temperatures) and to the latter only for leaching. Nitrogen oxides, when hydrated to acids, can attack the nitrocellulose polymer. Nitroesters can solvate and soften the adhesive. Neither is reversible in its effects.

3. Diesel and turbine fuels, hydraulic fluid, grease, heavy duty engine/transmission oil, and salt appear to have little or no damaging effects. CLP Cleaner, however, does cause adhesive joint deterioration and this material should not be used near combustible cartridge case munitions. NBC decontamination chemicals should be tested.

4. Aromatic hydrocarbons (such as xylene) do not appear to affect combustible cartridge case wall or adhesive, but ketones rapidly solvate the adhesive and cause disbonding. Degreasers such as methylethyl ketone should not be used near combustible cartridge case munitions.

5. The industrial pollutants sulfur dioxide and nitrogen dioxide do not cause deterioration under dry conditions. However, the corresponding acids can cause significant deterioration.

The statistical analysis of tensile strength data from the accelerated environmental exposure of full-up M829 rounds and from MAAP lot acceptance test data leads to the following conclusions:

1. Prediction models for tensile strength data based on accelerated testing conditions will have large confidence intervals on predicted values because of the large round-to-round variation (S_{rep} = 838 lbs). This result is independent of the model used for prediction.

2. The logistic prediction model is a good approximation of the observed data from the accelerated environmental exposure study. The shorter failure times than observed in field conditions indicates the time beyond which there is large uncertainty $0 \leq TS \leq 1051$ lbs.

3. The accelerated environmental exposure study suggests that disbonding of adhesive joints can occur rapidly if the right conditions for time, temperature, and relative humidity are reached. These results suggest the kinetics of adhesive joint behavior are not well understood. First-order, second-order, Arrhenius kinetic, etc. models may not provide improved tensile strength prediction until more information on the chemical properties of the adhesive joint bonding and the adhesive is known.

4. The increase in tensile strength variation from adaptor/case assemblies to full-up M829 rounds may indicate that the additional fabrications steps required for full-up M829 rounds introduce a significant amount of variability into the final skive joint strength.

5. Lot acceptance tests on adaptor/case assemblies cannot measure round-to-round variability in the full-up M829 rounds.

The results of this study suggest that future work should focus on achieving a better understanding of the properties of the joint adhesive and on improving the engineering and production of the skive joint.

Time-to-failure lifetime studies appear to be the main alternative to response surface modelling. This approach to predictive modelling of the M829 may meet with the same round-to-round variability as observed in this study, with the variability being exhibited as a wide distribution of the times required for failure (skive joint disbonding). It is suggested that if such a study is attempted, that the rounds be apportioned among the exposures according to the severity of the temperature or humidity stress (14). A greater number of rounds should be used in the less severe exposures where times to failure are likely to be long and differences among rounds magnified. Although the M829A1 has a considerably stronger skive joint (average of ca. 5,000 - 6,000 lbs), the standard deviation appears to be about the same, and models may have the same uncertainty as for the M829.

5 ACKNOWLEDGEMENT

The authors gratefully acknowlege Mr. Robert Kuper, Mrs. Silva Manjikian, Mr. Tom Brown, Mr. Henry Van Kyke III, and Dr. Eric Bixon of the Product Assurance Directorate at Picatinny Arsenal for many helpful discussions and guidance. Mr. Henry Van Kyke III supplied the sample of the CLP, and Dr. Jim Mengenhauser of the U.S. Army Mobility Equipment Research and Development Command at Fort Belvoir, Virginia provided the military specitications lubricants, hydraulic fluid, and grease.

6 REFERENCES

1. C. Y. Manning (November, 1987). Deterioration of 120-mm M829 Skive Joint in Storage, Technical Report ARAED-TR-87028, U.S. Army Research, Development and Engineering Center, Picatinny Arsenal, NJ.

2. C. Y. Manning (March, 1989). Nitrate Ester Migration from Propellant to Combustible Cartridge Case, American Defense Preparedness Association Meeting, Phoenix, AZ.

3. J. M. Hoegfeldt, R. E. Issleifson, and R. G. Wittmer (October 1984). Engineering Report ER 4561, Honeywell, Minneapolis, MN. Also earlier reports in this series.

4. L. Druet and M. Asselin (1988). A Review of Stability Test Methods for Gun and Mortar Propellants: The Chemistry of Propellant Ageing, J. of Energetic Materials, 6, 27-43.

5. G. E. P. Box and N. R. Draper (1987). Empirical Model-Building and Response Surfaces, John Wiley & Sons, New York.

6. E. J. Liebisch (October, 1989). Predictive Surveillance for Tank Ammunition. Effects of Air Pollutants on Tank Ammunition Materials. Oak Ridge National Laboratory, Oak Ridge, TN.

7. M. D. Osborne and J. Waineo (October 31, 1990). M1A1 Ammunition Compartment Temperature/Relative Humidity Study, Keweenaw Research Center, Michigan Technological University, Houghton, MI.

8. P. F. Krause (July, 1978). A Digest of High Temperature Storage Literature, U. S. Army Engineer Topographic Laboratories, Fort Belvoir, VA. Also, presentations by P. Chiodo, T. Brown, and D. G. Fernold, Jr., Predictive Technology Symposium - 91, National Conference of Predictive Technology, November 13-14, 1991, The Skylands Convention Center, Randolph, NJ.

9. Norman Draper and Harry Smith (1986). Applied Regression Analysis, Second Edition, John Wiley & Sons, NY.

10. D. M. Bates and D. G. Watts (1988). Nonlinear Regression Analysis & Its Applications, John Wiley & Sons, NY.

11. SAS Institute Inc. (1988). SAS/STAT™ User's Guide, Release 6.03 Edition., Cary, NC: SAS Institute Inc.

12. William R. Nance, Jr. (January 7, 1991). Personal Communication to Wayne H. Griest, Milan Army Ammunition Plant, Milan, TN.

13. C. -h Ho, W. H. Griest, and M. R. Guerin (December 31, 1991). Survey of Candidate Chemistries for Skive Joint Deterioration Indicator Strip, Oak Ridge National Laboratory, Oak Ridge, TN.

14. W. Q. Meeker amd G. J. Hahan (1985). How to Plan an Accelerated Life Test - Some Practical Guidelines. Volume 10, American Society for Quality Control, Milwaukee, WI.

15. C. Y. Manning (Oct., 1986). Nitroester Migration in M203A1 Propelling Charges for the 155mm Howitzer, Technical Report ARAED-TR-86035, U.S. Army Research, Development and Engineering Center, Picatinny Arsenal, NJ.

7 DISTRIBUTION LIST

Mr. Paul E. Chiodo, Acting Cheif Nuclear Systems and Stockpile Reliability Division Attention: SMCAR-QAN Picatinny Arsenal, NJ 07806-5000	25
Central Research Library Bldg. 4500N, MS-6191 Oak Ridge National Laboratory P.O. Box 2008 Oak Ridge, TN 37831-6191	1
Document Reference Section Bldg. 9711-1, MS-6107 Oak Ridge National Laboratory P.O. Box 2008 Oak Ridge, TN 37831-6286	1
Assistant Manager Energy Research and Development U.S. Department of Energy, Oak Ridge Operations P.O. Box E Oak Ridge, TN 37831-8600	1
W.H. Griest Bldg. 4500S, MS-6120 Oak Ridge National Laboratory P.O. Box 2008 Oak Ridge, TN 37831-6120	1
M.R. Guerin Bldg. 4500S, MS-6120 Oak Ridge National Laboratory P.O. Box 2008 Oak Ridge, TN 37831-6120	10
Mr. Robert J. Kuper, Chief Packaging Division SMCAR-AEP Picatinny Arsenal, NJ 07806-5000	1

Laboratory Records 3
Bldg. 4500N, MS-6120
Oak Ridge National Laboratory
P.O. Box 2008
Oak Ridge, TN 37831-6285

ORNL Patent Office 1
Bldg. 4500N, MS-6258
Oakf Ridge National Laboratory
P.O. Box 2008
Oak Ridge, TN 37831-6258

U.S. Department of Energy 2
Office of Scientific and Technical Information
P.O. Box 62
Oak Ridge, TN 37831

J.H. Cliff 1
Bldg. 9202, MS 8097
Martin Marietta Energy Systems, Inc., Y-12 Plant
P.O. Box 2009
Oak Ridge, TN 37831-8097

R.M. Davis 1
Bldg. 4500N, MS-6195
Oak Ridge National Laboratory
P.O. Box 2008
Oak Ridge, TN 37831-6195

C.K. Bayne 1
Bldg. 6011, MS-6370
Oak Ridge National Laboartory
P.O. Box 2008
Oak Ridge, TN 37831-6370

J.E. Caton 1
Bldg. 4500S, MS-6120
Oak Ridge National Laboratory
P.O. Box 2008
Oak Ridge, TN 37831-6120

R.H. Baldwin 1
Bldg. 4500S, MS-6155
Oak Ridge National Laboratory
P.O. Box 2008
Oak Ridge, TN 37831-6155

W.M. Caldwell 1
Bldg. 4500S, MS-6120
Oak Ridge National Laboratory
P.O. Box 2008
Oak Ridge, TN 37831-6120

W.M. Nance, Jr. 1
Martin Marietta Ordnance Systems, Inc.
Milan Army Ammunition Plant
Milan, TX 38358

A.M. Ammons 1
Bldg. 9202, MS-8096
Martin Marietta Energy Systems, Inc., Y-12 Plant
P.O. Box 2009
Oak Ridge, TN 37831-8096

J.H. Hannah 1
Bldg. 7601, MS-6304
Oak Ridge National Laboratory
P.O. Box 2008
Oak Ridge, TN 37831-6304

J.H. Moneyhun 1
Bldg. 4500S, MS-6120
Oak Ridge National Laboratory
P.O. Box 2008
Oak Ridge, TN 37831-6120

H. McCoy, Jr. 1
Bldg. 4500S, MS-6155
Oak Ridge National Laboratory
P.O. Box 2008
Oak Ridge, TN 37831-6155